NASA/TP-2000-209023

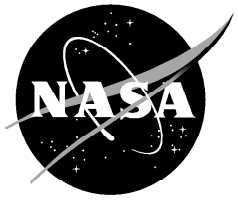

The SR-71 Test Bed Aircraft: A Facility for High-Speed Flight Research

Stephen Corda, Timothy R. Moes, Masashi Mizukami,
Neal E. Hass, Daniel Jones, Richard C. Monaghan,
Ronald J. Ray, Michele L. Jarvis, and Nathan Palumbo
NASA Dryden Flight Research Center
Edwards, California

June 2000

The NASA STI Program Office…in Profile

Since its founding, NASA has been dedicated to the advancement of aeronautics and space science. The NASA Scientific and Technical Information (STI) Program Office plays a key part in helping NASA maintain this important role.

The NASA STI Program Office is operated by Langley Research Center, the lead center for NASA's scientific and technical information. The NASA STI Program Office provides access to the NASA STI Database, the largest collection of aeronautical and space science STI in the world. The Program Office is also NASA's institutional mechanism for disseminating the results of its research and development activities. These results are published by NASA in the NASA STI Report Series, which includes the following report types:

- TECHNICAL PUBLICATION. Reports of completed research or a major significant phase of research that present the results of NASA programs and include extensive data or theoretical analysis. Includes compilations of significant scientific and technical data and information deemed to be of continuing reference value. NASA's counterpart of peer-reviewed formal professional papers but has less stringent limitations on manuscript length and extent of graphic presentations.

- TECHNICAL MEMORANDUM. Scientific and technical findings that are preliminary or of specialized interest, e.g., quick release reports, working papers, and bibliographies that contain minimal annotation. Does not contain extensive analysis.

- CONTRACTOR REPORT. Scientific and technical findings by NASA-sponsored contractors and grantees.

- CONFERENCE PUBLICATION. Collected papers from scientific and technical conferences, symposia, seminars, or other meetings sponsored or cosponsored by NASA.

- SPECIAL PUBLICATION. Scientific, technical, or historical information from NASA programs, projects, and mission, often concerned with subjects having substantial public interest.

- TECHNICAL TRANSLATION. English-language translations of foreign scientific and technical material pertinent to NASA's mission.

Specialized services that complement the STI Program Office's diverse offerings include creating custom thesauri, building customized databases, organizing and publishing research results…even providing videos.

For more information about the NASA STI Program Office, see the following:

- Access the NASA STI Program Home Page at ***http://www.sti.nasa.gov***

- E-mail your question via the Internet to help@sti.nasa.gov

- Fax your question to the NASA Access Help Desk at (301) 621-0134

- Telephone the NASA Access Help Desk at (301) 621-0390

- Write to:
  NASA Access Help Desk
  NASA Center for AeroSpace Information
  7121 Standard Drive
  Hanover, MD 21076-1320

NASA/TP-2000-209023

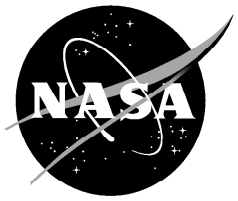

The SR-71 Test Bed Aircraft: A Facility for High-Speed Flight Research

Stephen Corda, Timothy R. Moes, Masashi Mizukami,
Neal E. Hass, Daniel Jones, Richard C. Monaghan,
Ronald J. Ray, Michele L. Jarvis, and Nathan Palumbo
NASA Dryden Flight Research Center
Edwards, California

National Aeronautics and
Space Administration

Dryden Flight Research Center
Edwards, California 93523-0273

June 2000

ABSTRACT

The SR-71 test bed aircraft is shown to be a unique platform to flight-test large experiments to supersonic Mach numbers. The test bed hardware mounted on the SR-71 upper fuselage is described. This test bed hardware is composed of a fairing structure called the “canoe” and a large “reflection plane” flat plate for mounting experiments. Total experiment weights, including the canoe and reflection plane, as heavy as 14,500 lb can be mounted on the aircraft and flight-tested to speeds as fast as Mach 3.2 and altitudes as high as 80,000 ft. A brief description of the SR-71 aircraft is given, including details of the structural modifications to the fuselage, modifications to the J58 engines to provide increased thrust, and the addition of a research instrumentation system. Information is presented based on flight data that describes the SR-71 test bed aerodynamics, stability and control, structural and thermal loads, the canoe internal environment, and reflection plane flow quality. Guidelines for designing SR-71 test bed experiments are also provided.

NOMENCLATURE

C_D	coefficient of drag
C_l	rolling moment coefficient
C_{l_β}	dihedral effect, $\partial C_l / \partial\beta$, deg^{-1}
C_m	pitching-moment coefficient
C_{m_α}	longitudinal static stability derivative, $\partial C_m / \partial\alpha$, deg^{-1}
$C_{m_{\delta_e}}$	elevon control effectiveness derivative, $\partial C_m / \partial\delta_e$, deg^{-1}
C_{m_0}	coefficient of pitching moment at zero lift
C_n	yawing moment coefficient
C_{n_β}	directional static stability, $\partial C_n / \partial\beta$, deg^{-1}
$C_{n_{\delta_r}}$	yawing moment caused by rudder derivative, $\partial C_n / \partial\delta_r$, deg^{-1}
C_Y	side force coefficient
C_{Y_β}	side force caused by sideslip derivative, $\partial C_Y / \partial\beta$, deg^{-1}
KEAS	equivalent airspeed, knots
LASRE	Linear Aerospike SR-71 Experiment
$\bar{q}$	dynamic pressure, lbf/ft^2
$P_{t_{max}}$	maximum total pressure, lbf/ft^2
$P_{t_{min}}$	minimum total pressure, lbf/ft^2
P_{t_∞}	free-stream total pressure, lbf/ft^2
ref	aerodynamic moment derivatives corrected to 25-percent mean aerodynamic chord
S	SR-71 reference area, 1605 ft^2
SAS	stability augmentation system
W	weight, lb

α wing reference plane angle of attack, deg

β angle of sideslip, deg

δ_e elevon deflection, $\delta_e = -(\delta_e\,(\text{left inboard}) + \delta_e\,(\text{right inboard}))$, deg (positive is trailing edge down)

δ_r rudder deflection, $\delta_r = -(\delta_r\,(\text{left}) + \delta_r\,(\text{right}))$, deg (positive is trailing edge left)

INTRODUCTION

The SR-71 test bed aircraft (fig. 1) at the NASA Dryden Flight Research Center (Edwards, California) provides a unique capability to conduct flight research from subsonic speeds to high supersonic Mach numbers and high altitudes. Structural modifications to the SR-71 upper fuselage allow for the carriage of a large external payload on top of the aircraft. The maximum external payload weight that can be carried on the aircraft is 14,500 lb. The weight of the test bed structure currently on the aircraft is approximately 9,200 lb.

A large fairing structure, the "canoe," is mounted on the SR-71 upper fuselage (fig. 2). The canoe provides volume for the packaging of experiment equipment and systems. A large flat-plate structure, the "reflection plane," is mounted on top of the canoe. Another structure, the "kayak," inclines the reflection plane at approximately a –2° angle relative to the SR-71 upper fuselage. This inclination approximately aligns the reflection plane with the local flow. The reflection plane provides a flat surface for experiment placement and can also serve as a flow symmetry plane.

EC99-45102-03

Figure 1. NASA SR-71A test bed aircraft.

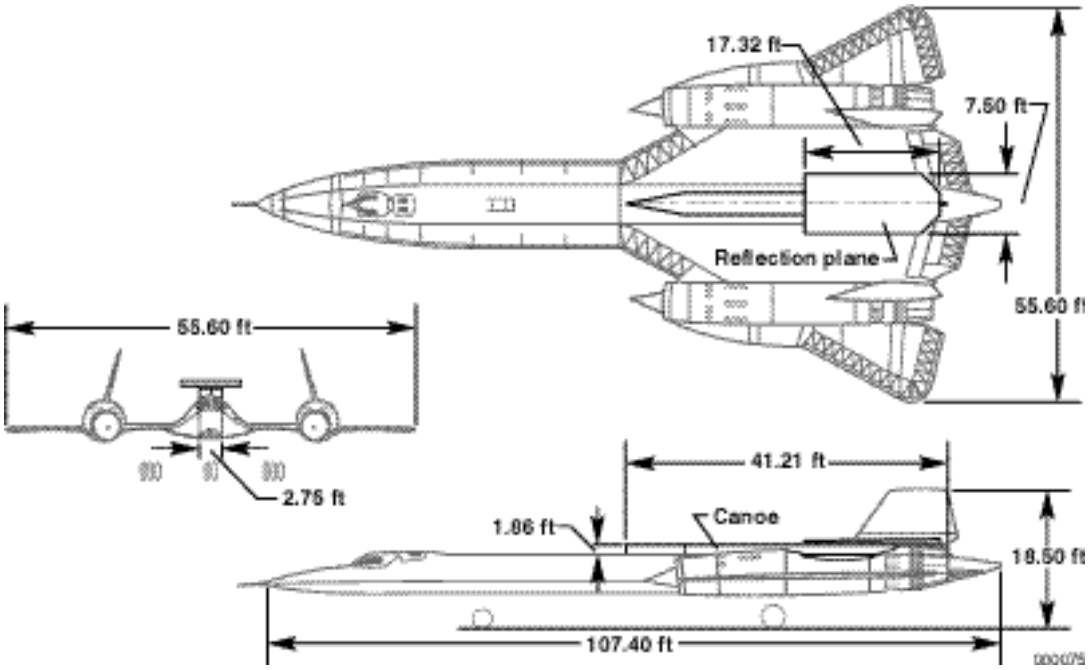

(a) Canoe and reflection plane mounted on the SR-71 aircraft.

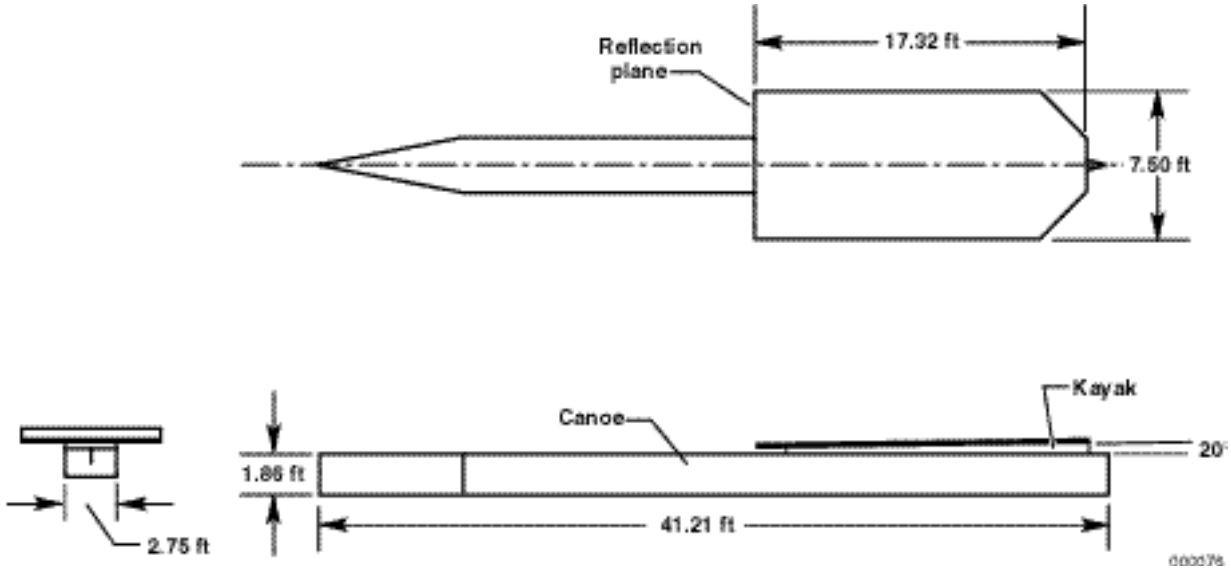

(b) Canoe and reflection plane geometry.

Figure 2. Canoe and reflection plane.

The canoe, kayak, and reflection plane are structures used in a previous flight test program, the Linear Aerospike SR-71 Experiment (LASRE). The LASRE was a captive-carry flight test of a linear aerospike rocket engine mounted atop the SR-71 aircraft (ref. 1). The aerospike rocket engine was integrated in a semispan lifting-body shape called the "model." In the LASRE configuration, the canoe, kayak, reflection plane, and model were collectively identified as the "pod." The model was mounted on the reflection plane. The model housed the liquid oxygen tank and other systems for the rocket engine. Tanks for gaseous hydrogen fuel and engine cooling water were located in the canoe.

A research instrumentation system was installed for the LASRE experiment that is capable of both onboard recording and telemetering research data. Currently, the SR-71 aircraft is in flyable storage at NASA Dryden. The aircraft can be returned to flyable status in a few months.

This paper provides technical information for potential experimenters about the capabilities of the NASA SR-71 test bed aircraft. This information supplements the technical information about the basic SR-71 aircraft provided in reference 2. A description is given of the basic SR-71 aircraft, structural modifications, canoe and reflection plane structures, SR-71 propulsion system, and research instrumentation system. Information concerning the design of the SR-71 test bed experiments is given in the appendix. Flight data are presented from the test bed flights in the areas of aerodynamics, stability and control, structural loads, thermal loads, the canoe internal environment, and the flow quality on the reflection plane. Some guidelines for designing SR-71 test bed flight experiments are also provided.

SR-71 TEST BED DESCRIPTION

The NASA SR-71 aircraft has been modified to be used as a high-speed test bed aircraft. The following sections describe the SR-71 aircraft, aircraft structural modifications, canoe and reflection plane, aircraft propulsion system and modifications, and flight research instrumentation and data acquisition system.

Aircraft Description

NASA has an SR-71 aircraft at the NASA Dryden Flight Research Center that is operated as a flight research aircraft. This SR-71 test bed flight research aircraft is a modified SR-71A aircraft and has been assigned NASA aircraft tail number 844. The SR-71A aircraft, designed and manufactured by the Lockheed Advanced Development Company (Palmdale, California), has a tandem, two-place cockpit configuration with flight controls in the forward cockpit only. A flight test engineer occupies the aft cockpit and typically controls the experiment and operates emergency systems, in addition to performing normal radio and navigation duties. The SR-71 aircraft has a rather narrow flight envelope; maximum cruise performance is approximately Mach 3.2 at altitudes higher than 80,000 ft (fig. 3). The aircraft has titanium construction and is painted black to operate at the high temperatures associated with Mach-3 flight (hence its designation as the "Blackbird"). Table 1 shows general specifications of the SR-71A aircraft.

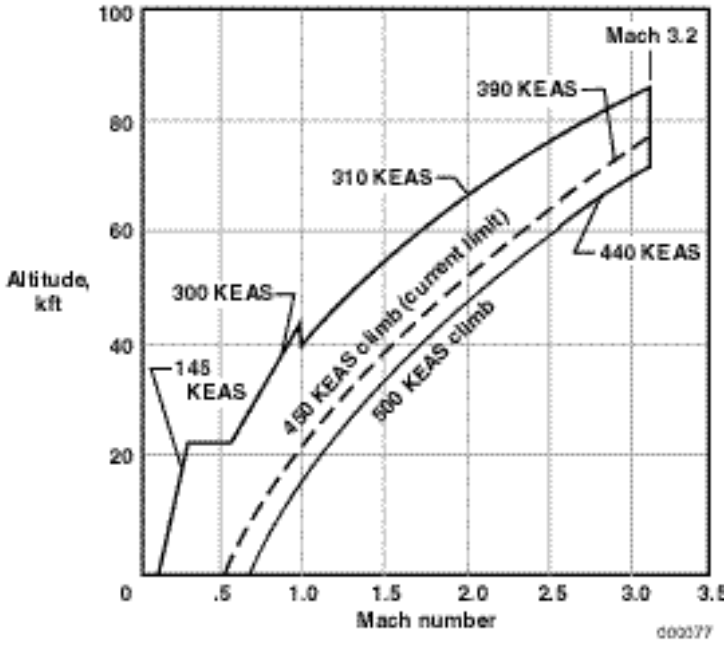

Figure 3. SR-71A test bed flight envelope.

Table 1. SR-71A test bed configuration specifications.

Item	Specification
Aircraft length	107.40 ft
Aircraft wing span	55.60 ft
Aircraft height	18.50 ft
Wing reference chord (also mean aerodynamic chord)	37.70 ft
Gross takeoff weight	143,000 lb
Basic aircraft zero fuel weight	59,000 lb
Canoe, kayak, and reflection plane weight	9,200 lb
Fuel	JP-7
Design Mach number	3.2
Canoe length	41.20 ft
Canoe width	2.75 ft
Canoe height	1.86 ft
Reflection plane length	17.30 ft
Reflection plane width	7.50 ft

Installation of experiments on top of the SR-71 aircraft limits performance because of reduced fuel load and increased aerodynamic drag. A high-speed flight mission of the test bed aircraft normally would include a takeoff with approximately 35,000 lb of fuel followed shortly by in-flight refueling at an altitude of 20,000 ft. During the LASRE program, the SR-71 internal fuel tank floats were adjusted to limit the usable internal fuel capacity to approximately 67,000 lb. This adjustment was done to prevent exceeding the aircraft total weight limit while carrying the approximately 14,500 lb LASRE experiment. Also, 5,000 lb of fuel in the most forward aircraft fuel tank was considered unusable during the LASRE program as that amount of fuel was required to offset the aft center of gravity of the LASRE hardware. During the test bed program with the LASRE model removed, only 1,200 lb of fuel were considered unusable for center-of-gravity considerations. For future flight programs, the fuel tank floats can be adjusted to increase usable fuel tank capacity if total weight and center-of-gravity constraints are satisfied.

Aircraft Structural Modifications

Modifications were made to the SR-71 structure to carry the experiment hardware for the LASRE. The aircraft structural modifications included strengthening the aircraft fuselage and installing attachment hardware to the upper fuselage. The structural attachment points consist of a forward, self-aligning ball, and two vertical links and one lateral link on the aft upper fuselage. These attachment locations do not affect the normal load paths or stiffness of the basic SR-71 aircraft. The concentrated load points at the attachments required local reinforcement internal to the fuselage to distribute flight loads into the SR-71 airframe. To eliminate the need for structural testing, all new structure and existing modified structure used a factor of safety of 2.25, 50-percent greater than the normal SR-71 aircraft design factor of safety of 1.50.

Canoe and Reflection Plane Description

Figure 2 shows the canoe and reflection plane structures. The canoe is 41.20 ft long, 2.75 ft wide, 1.86 ft tall, and 2.00 in. thick. The reflection plane is 17.3 ft long and 7.5 ft wide. Both structures are constructed of common low-carbon steel. These structures were designed with a factor of safety of 2.25. As previously mentioned, the canoe is mounted between the SR-71 twin vertical rudders at three hard points on the SR-71 fuselage. The canoe and reflection plane are designed to remain attached to the SR-71 aircraft and cannot be jettisoned or released in flight. Table 2 shows the weights for the LASRE and test bed configurations.

A nitrogen purge system, supplied by fuselage-mounted Dewar flasks, has been installed in the canoe. The canoe internal volume may be purged with inert, nitrogen gas for several reasons. The primary purpose may be to minimize the presence of oxidizer if flammable stores are carried within the canoe volume. Oxidizer sources can be either air that has infiltrated from the outside or leakage from any onboard oxidizer feed systems. The secondary purpose of the inert purge may be to dilute any leaking volatiles, carried for a particular experiment, to below flammability limits and to transport the mixture from inside the canoe to the outside using vent ports. Ignition sources also can be reduced by nitrogen purging of the electronics boxes, valves, and so forth. The onboard nitrogen purge system can be easily modified to service other experiment requirements and configurations.

The gaseous nitrogen is supplied from two liquid nitrogen Dewar flasks onboard the SR-71 aircraft. The liquid nitrogen is vaporized by electric heaters and dispersed into the canoe volume through perforated “piccolo” tubes.

Table 2. LASRE and test bed weight breakdown.

Component	LASRE weight, lb[a]	Test bed weight, lb[b]
Model assembly	4,300	None
Canoe structure	4,100	4,100
Kayak structure	300	300
Reflection plane structure	2,000	2,000
Hydrogen tanks	700	700
Helium tanks	200	200
Water tanks	600	600
Water	800	None
Electrical	200	200
Plumbing	300	300
Paint and ablative	100	100
Skirts	100	100
Unaccounted for weight growth	600	600
TOTAL	14,300	9,200

a. Total LASRE weight measured before installation on SR-71 aircraft.

b. Test bed total weight calculated from weight allocations in table.

The two Dewar flasks hold a total of 100 L (180 lb) of liquid nitrogen. The flow rate presently is metered to 34 standard ft^3/min. This setting provides an operational duration of approximately 90 min. At these flow rates, the volume changeout rate is approximately 0.33 volume changeouts/min on the ground, and 2.00 changeouts/min at an altitude of 65,000 ft.

For ground operations, an external nitrogen gas source may be used to conserve the onboard supply and provide for a larger ground operations purge mass flow rate. During flight, the purge flow can be controlled from the SR-71 rear cockpit, and the nitrogen gas source operating pressure is telemetered to the ground to verify operation.

Approximately 20 gal of water are carried aboard the SR-71 aircraft for cooling of experiment electronics and instrumentation. The recirculating coolant flow rate through the electronics and instrumentation is approximately 3 gal/min. The water is chilled by cold air from the SR-71 environmental control system. The system has significant margin for cooling additional equipment beyond the current instrumentation system usage.

Thermocouples are distributed within the canoe for local fire detection and to monitor canoe internal temperatures. Certain components, such as the composite-wrapped hydrogen tanks that were employed by LASRE, the electronic control systems, and the instrumentation signal-conditioning boxes, are temperature-limited and require some means to monitor their exposure.

Aircraft Propulsion System Description and Modifications

The SR-71 propulsion system has three primary components: variable geometry, axisymmetric, mixed-compression inlets; two turbojet engines with afterburners; and airframe-mounted, convergent-divergent, blow-in-door ejector nozzles (ref. 3). The SR-71 aircraft is powered by two 34,000-lbf–thrust class J58 afterburning turbojet engines (Pratt & Whitney, West Palm Beach, Florida). At speeds faster than Mach 2.2, some of the airflow is bled from the fourth stage of the compressor and dumped into the augmentor inlet using six bleed-bypass tubes, circumventing the core of the engine and transitioning the propulsive cycle from a pure turbojet to a turbo-ramjet. The engine is hydromechanically controlled and burns a special low-volatility jet fuel mixture known as JP-7.

Thrust Enhancement Concepts

Pratt & Whitney was asked to analytically evaluate several options for increasing the thrust of the J58 engine (ref. 4) to provide enhanced vehicle performance for carrying external payloads. The enhancements considered included increasing turbine exit total temperature, increasing compressor rotor speed, modifying the compressor bleed and inlet guide vane schedules, and increasing the augmentor fuel flow combined with oxidizer injection. Only the increased turbine exit temperature and increased rotor speed enhancements have been implemented to date.

Engine Control Modifications

The NASA Dryden requirement is that the thrust enhancements do not decrease the engine life (time between overhaul) to less than 50 hr. Pratt & Whitney estimated that a combination of a 150-r/min rotor speed increase and a 75 °F turbine exit total temperature increase would satisfy this engine life requirement. In fact, through flight evaluation of the thrust enhancement, the 50-hr overhaul requirement has been relaxed to a 50-hr inspection. Both changes involved relatively simple in-the-field, mechanical adjustments to the engine main fuel control. As figure 4 shows, the rotor speed and turbine temperature increases resulted in a predicted net thrust increase of an average 5 percent throughout the Mach range.

To further assure the best performance available, the engine manufacturer was asked to select a set of top-performing J58 engines for the SR-71 test bed aircraft. Several engines were evaluated on a static ground test stand until two primary engines were identified to best meet the performance requirements. In addition, a third engine was identified as a spare. These engines have been trimmed to their maximum normal operating band with respect to airflow and exhaust gas temperature.

Although not currently implemented, the augmentor fuel control could also be mechanically adjusted to increase the afterburner fuel flow by approximately 4 percent throughout the Mach range. This extra fuel flow could take advantage of additional oxidizer available from other enhancements such as nitrous

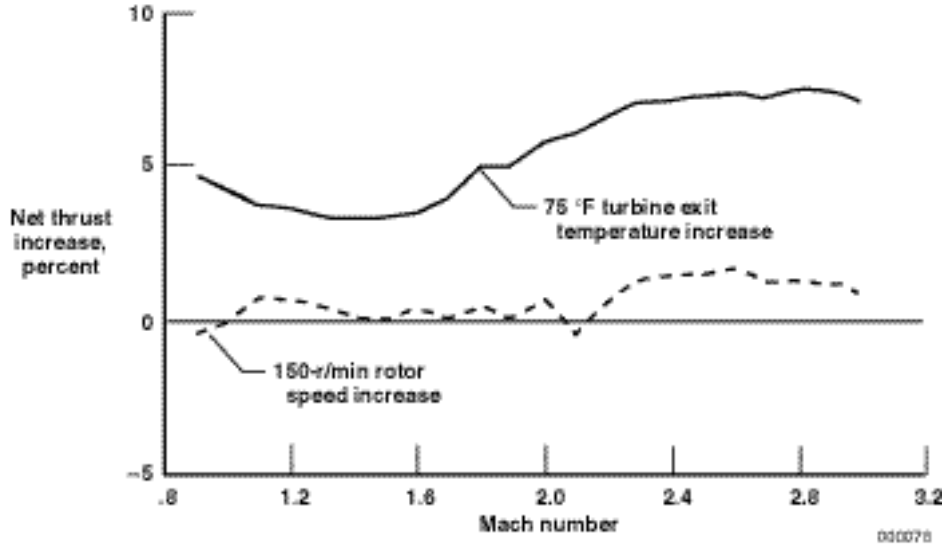

Figure 4. Net thrust increase caused by thrust enhancement.

oxygen injection (as described in reference 5), providing additional thrust. These modifications are predicted to provide an additional 5-percent thrust increase across the flight envelope.

Flight Research Instrumentation and Data Acquisition System

Figure 5 shows the SR-71 test bed instrumentation system layout. Three pulse code modulation encoders on board the SR-71 test bed aircraft are configured as one master with two remotes. The encoder model used is a modular microminiature signal conditioner and pulse code modulation encoder. Each encoder can be configured to accommodate various sensors using the different types of modules

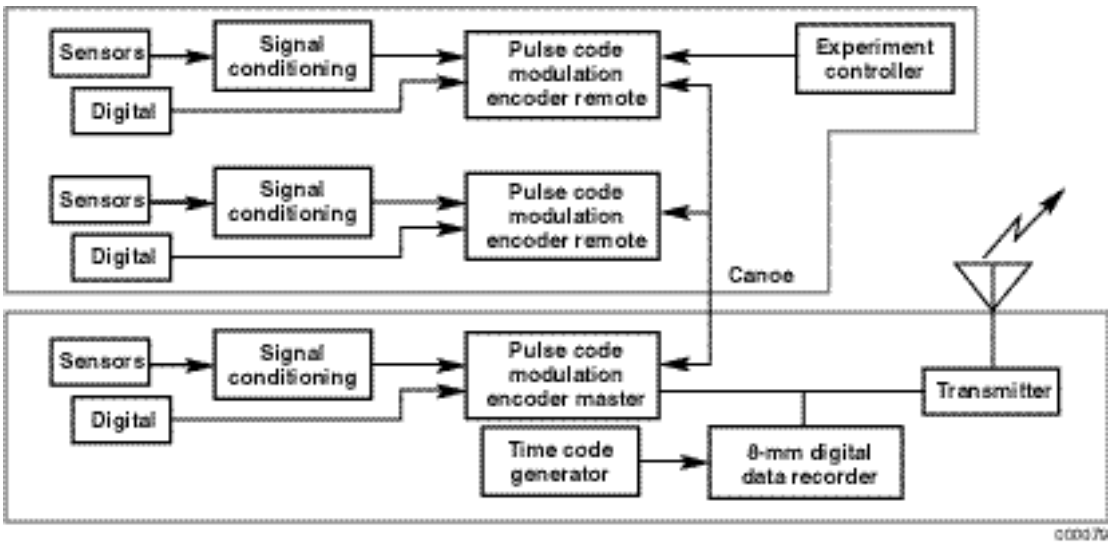

Figure 5. SR-71 test bed instrumentation system layout.

available from the vendor. The master encoder is located in the SR-71 fuselage chine bay and the two remote encoders are located in the canoe.

Currently, the system has 12-bit resolution and is configured to run at 800 kbits/sec, giving a maximum sample rate of 400 samples/sec. This capability can be increased as required by a specific experiment. The data can be transmitted from the aircraft to the ground and also can be digitally recorded onboard the aircraft.

NASA-designed signal-conditioning boards are provided for the front end of each analog channel. These signal-conditioning boards contain instrumentation amplifiers with gain and offset control and filters. Excitation for strain gage–type sensors or resistance temperature devices can be provided through these signal-conditioning boards.

The current measurement capabilities located within the aircraft include 112 analog signals, 8 serial data streams, and 4 12-bit digital data words or equivalent discrete measurements. Signal conditioning can be provided for most types of transducers including strain gage, pressure, resistance, temperature, position, and acceleration. Single-ended and differential drivers can be provided for the eight serial data streams.

Current aircraft measurements include aircraft airdata, control surface positions, linear accelerations, angular rates, inertial attitudes, fuel system data, and J58 engine data. Aircraft airdata are composed of angle of attack, angle of sideslip, total pressure, static pressure, Mach number, airspeed, and total temperature. Control surface positions include the position of the elevons, rudders, engine inlet spikes, engine bypass doors, and throttles. Normal and longitudinal linear acceleration and pitch rate are measured at fuselage stations 234.5 (near the cockpit) and 683.0. Roll and yaw angular rates are also measured at fuselage station 683. Fuel system data include the six individual fuel tank quantities and center of gravity. Engine data are composed of the nozzle area, exhaust gas temperatures, and engine speed. The cooling-water temperatures for the aircraft instrumentation system are also measured.

The instrumentation system in the canoe consists of 224 analog signals, 16 serial data streams, and 8 12-bit digital data words or equivalent discrete measurements. Signal conditioning can be provided for most types of transducers including strain gage, pressure, resistance, temperature, position, and acceleration.

Current measurement capabilities in the canoe include pressures, temperatures, and strains. Typical pressure measurements are for gas storage tanks, feed lines, and the internal canoe environment. Multiplexed, electronic scanning pressure sensors are also available for measurements such as flow-field surveys, boundary-layer rakes, and local airdata probes. Temperatures typically measured include gas storage tank and internal canoe environment temperatures. The reflection plane has limited strain-gage instrumentation installed. A nine-hole hemispherical tip probe, which has static-pressure ports, is located on top of the canoe, forward of the reflection plane.

Figure 6 shows an oxygen sensor system installed in the canoe. The purpose of these sensors is to determine purge inert effectiveness, detect infiltration of outside air, and indicate the presence of any leaked oxidizer that may be carried. Each sensor has been calibrated and is temperature-controlled to reduce thermal drift of the sensor output. These sensors are point measurements that will not detect air or oxygen that may become trapped in other areas, but the number and distribution of the sensors are judged to be sufficient to characterize overall oxygen levels in the canoe. Accuracy of the sensor at sea level,

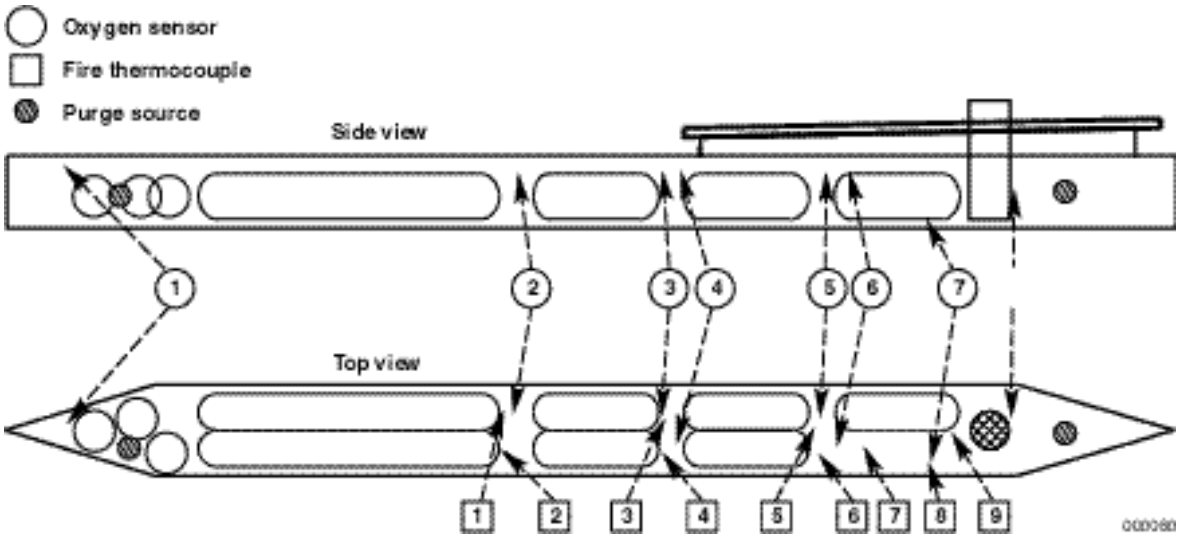

Figure 6. Location of oxygen sensors, fire thermocouples, and purge sources in canoe.

according to the specification sheet, is 1 percent, but calibration and correction determined an uncertainty that was much better than specified (ref. 6).

FLIGHT TEST DATA

Several SR-71 test bed flights were conducted to obtain baseline data for this configuration. Flight test results are given in the areas of aerodynamics and stability and control, structural and thermal loads, canoe internal environment, and reflection plane flow quality.

Aerodynamics and Stability and Control

Flight test analysis and results are presented for the SR-71 performance, transonic pitching moment, longitudinal stability and control, and lateral-directional stability and control. Guidance is provided in the area of stability and control for the design of new configurations for the SR-71 test bed.

SR-71 Performance

The added aerodynamic drag of an experiment is most critical in the transonic acceleration, where excess thrust is at a minimum. Poor transonic acceleration can affect the maximum Mach number attainable because less fuel is available for the acceleration. The maximum possible Mach number for the LASRE configuration was never determined. The maximum Mach number flown in the LASRE configuration was approximately Mach 1.8, which was achieved on a day with approximately a “standard day” temperature profile. Analysis has shown that Mach 2.5 could have been reached on that day with the available fuel. On “hot” days—that is, when the profile for temperature as a function of altitude is well above the standard day profile—the J58 engine thrust is significantly reduced, thereby significantly reducing the maximum Mach capability. The SR-71 test bed configuration (with no experiment mounted on the reflection plane) successfully reached Mach 3.0 on a “hot” day.

The drag increment caused by the entire LASRE pod was not measured in flight. However, the drag component caused by the LASRE model was measured using an in-flight force balance. This measurement did not include interference drag between the model and the remainder of the aircraft. Figure 7 shows the drag caused by the LASRE model measured by the force balance and extrapolated from Mach 1.8 to Mach 3.2 using standard supersonic aerodynamic theory assumptions. Figure 7 also shows the wind tunnel–predicted drag caused by the entire LASRE pod (ref. 7). Based on the LASRE flight data, future experiments that require flight at Mach numbers greater than Mach 2.5 should have a drag coefficient less than that measured for the LASRE model. However, other factors such as area ruling and shock interference that may affect the total drag of the configuration should be kept in mind.

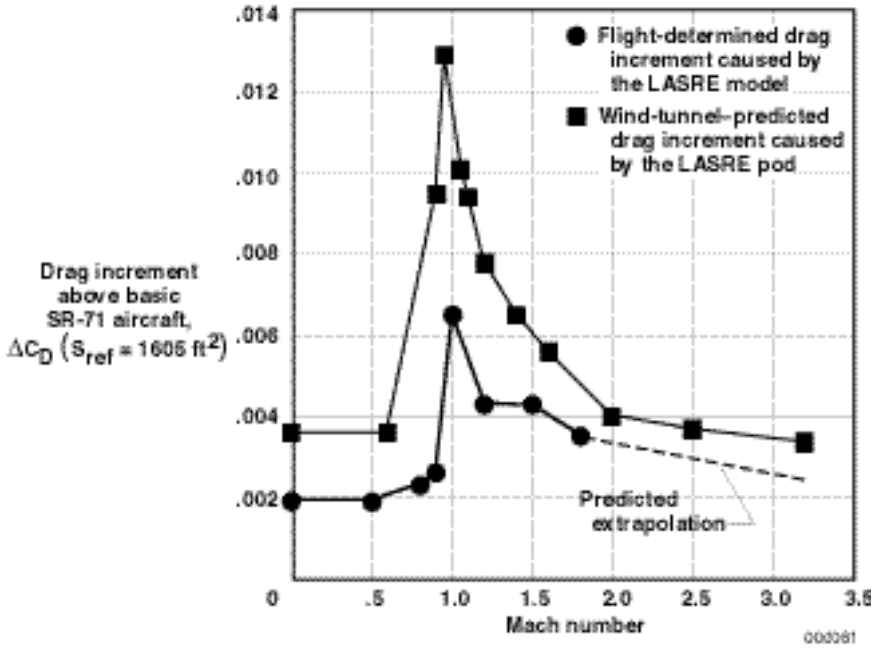

Figure 7. Drag increment predicted for the LASRE pod and LASRE model drag increment measured in flight using the force balance.

Transonic Pitching Moment

For the LASRE and test bed configurations, the transonic zero-lift pitching moment was significantly different than that of the baseline SR-71 aircraft configuration. With the wings level, accelerating flight test maneuvers were used to determine the incremental change in zero-lift pitching moment caused by these configurations as compared to the baseline aircraft. Reference 8 describes the analysis used to compute the zero-lift pitching-moment increment.

Figure 8 shows a plot of the flight-determined zero-lift pitching-moment increment for the modified configurations. Both configurations caused a subsonic nosedown pitching-moment increment and a noseup pitching-moment increment peak at approximately Mach 0.95. At supersonic Mach numbers less than approximately 1.7, the test bed configuration caused a significant nosedown increment. The test bed configuration required an additional 6° of noseup elevon trim compared to the LASRE at Mach 1.1, resulting in a significant increase in trim drag for the test bed configuration. These data show that the LASRE model contributed a positive pitching-moment increment. Similarly, most future experiments

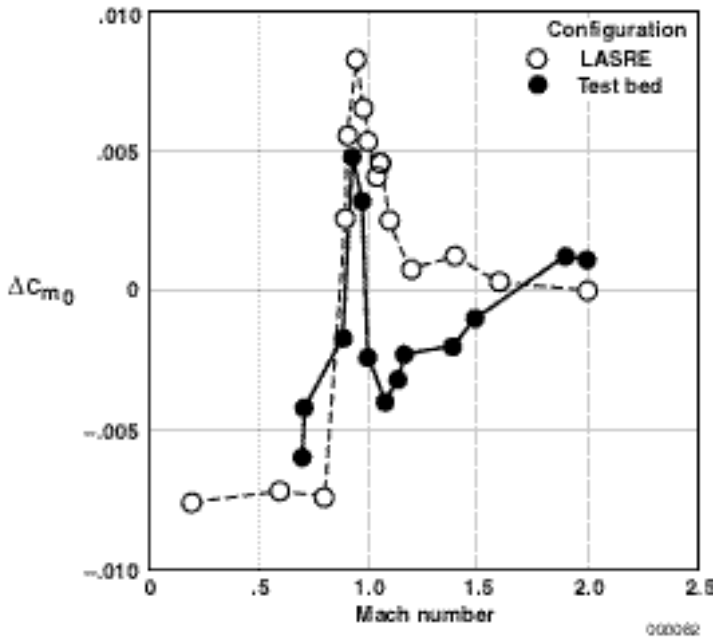

Figure 8. Zero-lift pitching-moment increments for the LASRE and SR-71 test bed configurations.

mounted on the reflection plane probably will also contribute a positive pitching moment, which will improve transonic performance by reducing trim drag caused by required noseup trim.

Stability and Control Analysis and Results

Extensive flight test has been completed to assess the changes in aircraft stability and control caused by the addition of experiments on the SR-71 upper fuselage. Flight data have been obtained for the baseline SR-71 aircraft to a maximum speed of Mach 2.9, for the LASRE configuration to a maximum of Mach 1.75, and for the test bed configuration to a maximum of Mach 3.0. An output-error parameter estimation program known as pEst was used to estimate the open-loop stability and control derivatives from pilot-input doublet maneuvers (refs. 9–10). The aircraft stability augmentation systems (SASes) were used in all axes during the pEst maneuvers to increase the closed-loop stability. Also, the engine inlets and bypass doors were operated in automatic mode during all test maneuvers. Reference 8 provides initial flight test results for the baseline SR-71 aircraft and the LASRE configuration. As is normally the case, longitudinal and lateral-directional maneuvers were performed and analyzed separately.

Figure 9 shows the stability and control flight test points analyzed and presented in this report. As the figure shows, the majority of the supersonic data were obtained at 450 knots equivalent airspeed (*KEAS*), which was the maximum speed cleared for the LASRE and test bed flight tests.

Longitudinal Stability and Control

Pitch doublet maneuvers were flown at the test conditions shown in figure 9 to obtain the longitudinal stability and control derivatives. Figures 10 and 11 show the longitudinal static stability derivative, C_{m_α}, and the elevon control effectiveness derivative, $C_{m_{\delta_e}}$, respectively, obtained from flight data. Flight

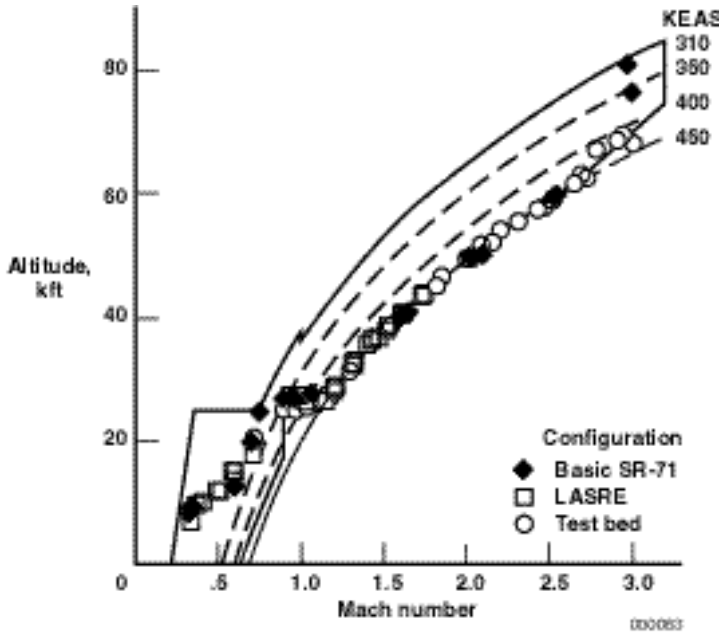

Figure 9. Flight conditions for stability and control test points.

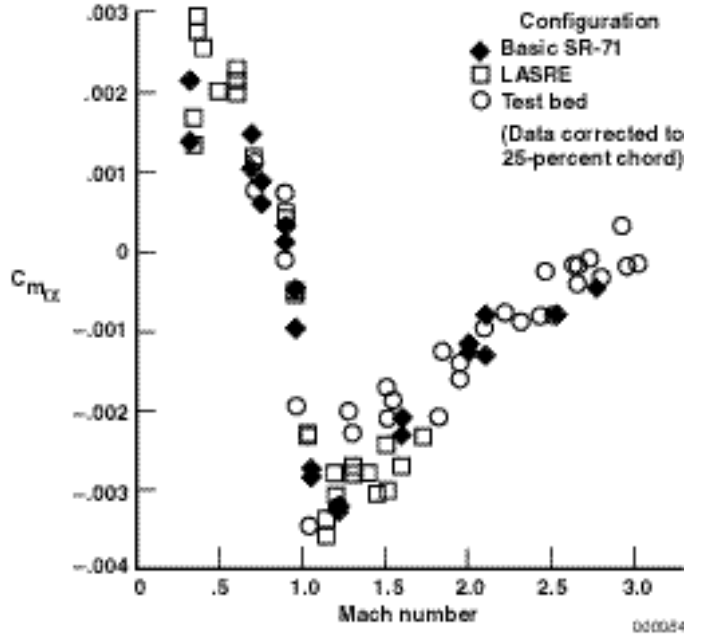

Figure 10. Flight-determined longitudinal static stability.

data were obtained at center-of-gravity locations ranging from 17.3 to 25.5 percent of the mean aerodynamic chord. However, all $C_{m_{\delta_e}}$ and C_{m_α} results were corrected to a common moment reference point at 25-percent mean aerodynamic chord. Figure 10 shows that the LASRE and test bed hardware had a negligible affect on the longitudinal static stability. Similarly, minimal effect existed on elevon control effectiveness except during subsonic flight in the LASRE configuration in which the control effectiveness was slightly reduced (fig. 11).

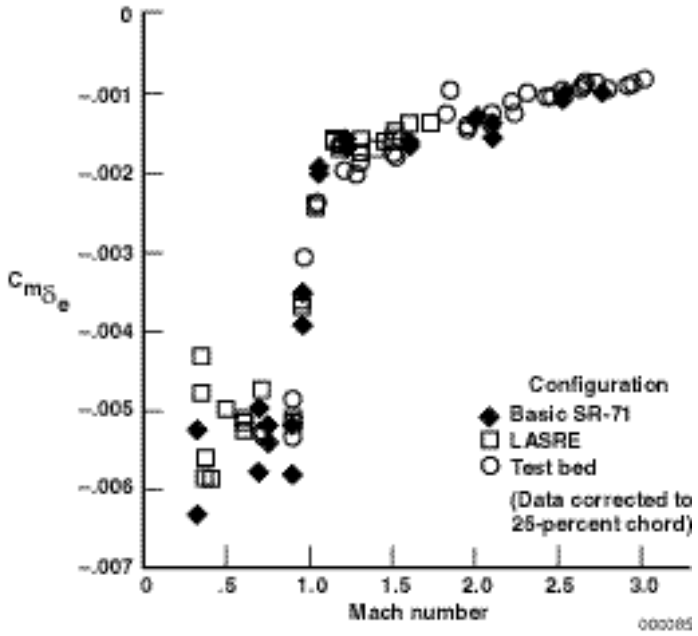

Figure 11. Flight-determined elevon control effectiveness.

Lateral-Directional Stability and Control

Yaw and roll doublet maneuvers were flown to obtain the lateral-directional stability and control derivatives. Directional static stability, C_{n_β}, and dihedral effect, C_{l_β}, were affected by the LASRE and test bed hardware as shown in figures 12 and 13, respectively. Directional stability data were corrected to a common 25-percent mean aerodynamic chord. Rudder effectiveness and aileron control effectiveness were not significantly affected by the LASRE or test bed experiments.

The baseline SR-71 aircraft was designed to have minimum (but still positive) open-loop directional static stability, C_{n_β}, at Mach 3.2. In addition, a directional SAS was required to provide acceptable handling qualities and to prevent extreme sideslip transients caused by inlet "unstarts." The yaw SAS uses yaw rate feedback for damping and lateral acceleration to augment stability. The effective closed-loop directional static stability provided by the yaw SAS can be computed using the following equation:

$$C_{n_\beta}(\text{Closed Loop}) = C_{n_\beta}(\text{Open Loop}) + C_{n_{\delta_r}} \frac{\bar{q}S_{ref}}{W} C_{Y_\beta}$$

A roll SAS is also used, although it basically provides only roll damping through roll rate feedback.

The open-loop directional static stability, C_{n_β}, showed reductions caused by the LASRE configuration and further reductions for the test bed configuration (fig. 12). Also plotted on figure 12 is the calculated closed-loop static stability for the test bed data to demonstrate the effectiveness of the yaw SAS. At approximately Mach 2.1, the test bed open-loop directional stability began decreasing rapidly toward 0 and then leveled off near 0. This decrease was a significant concern during the envelope expansion phase of the test bed flight program. Although less of a concern, the dihedral effect was also reduced (fig. 13). With the SAS on, piloted simulations were flown to determine the effect of reduced open-loop C_{n_β} and C_{l_β} on handling qualities and the aircraft responses caused by single engine failures

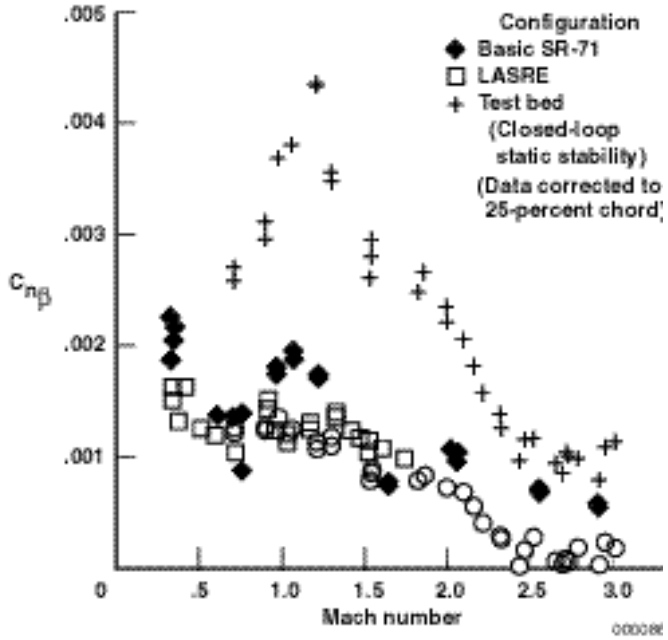

Figure 12. Flight-determined directional static stability.

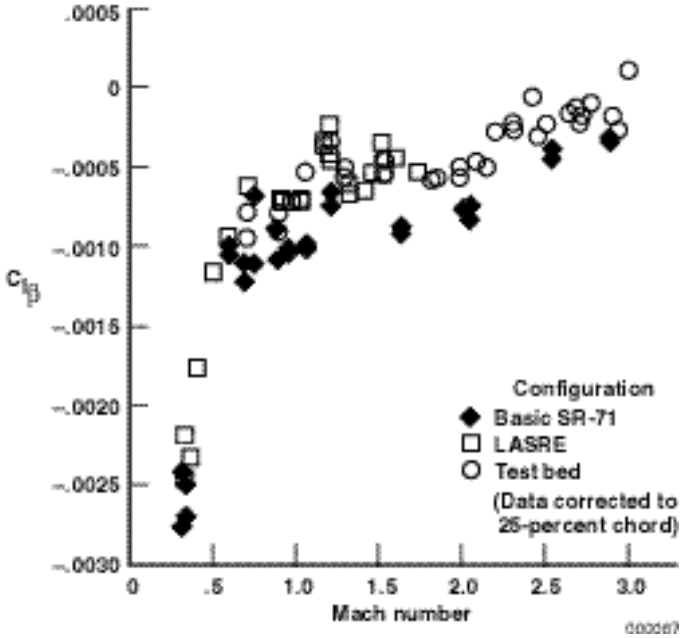

Figure 13. Flight-determined dihedral effect.

(for example, inlet “unstarts”). With reduced directional stability, an engine failure could result in significant sideslip leading to aircraft structural failure. With the SAS on, simulations were flown to determine the open-loop directional stability level that would result in exceeding the aircraft sideslip limit for an “engine out” situation. For the test bed configuration, this sideslip limit is the same as the limit for the baseline aircraft. The critical structural elements are the vertical tails for which a sideslip limit of 5.7° was used. The stability for Mach-3.2 flight was determined to be acceptable for the test bed configuration; however, the aircraft center of gravity was required to be forward of 23-percent mean aerodynamic chord for flight faster than Mach 2.5.

In the flight simulation, a lower limit for open-loop directional static stability of –0.0006 was established, which would be acceptable in the event of an “unstart” with the SAS operating. However, because of uncertainties in the simulation, a future program getting approved to fly with negative open-loop directional static stability is doubtful.

New Configurations

Stability and control derivatives have been obtained for the baseline SR-71 aircraft, the LASRE configuration, and the test bed configuration. For the LASRE program, extensive wind-tunnel tests were completed to obtain the stability and control derivative increments caused by the LASRE experiment. Based on the flight data obtained for the LASRE and test bed configurations, wind-tunnel data may not be required for future configurations.

This flight data set can be used to bound the stability and control effects of a new configuration mounted on the reflection plane. As figures 10 and 11 show, only slight changes in longitudinal stability and control were evident. Directional static stability and dihedral effect are reduced for both the LASRE and test bed configurations. The canoe is suspected to be the cause of this reduced C_{n_β} and the LASRE model to have had a positive effect on C_{n_β}. Therefore, any experiment mounted on the reflection plane would likely improve the directional stability over that of the test bed configuration. A stability and control flight envelope expansion approach would be required for any new configuration. The amount of envelope expansion required would likely increase with the physical size of the experiment.

Structural and Thermal Loads

Several SR-71 flights were flown in the LASRE and test bed configurations to investigate the structural envelope relating to the canoe attachment loads into the SR-71 aircraft. The critical flight loads were on the aft vertical links that attach the canoe to the SR-71 fuselage hard points (fig. 14). Data were gathered for the LASRE configuration at a weight of 14,320 lb with the center of gravity at fuselage station 1054.6, and for the test bed configuration at a weight of 9,151 lb with the center of gravity at fuselage station 1038.0.

For the LASRE and test bed flights, the left aft vertical link of the canoe experienced slightly higher loads than the right aft vertical link. Figure 14 shows measured loads on the left aft vertical link. The LASRE loads flight data were generated by steady-state sideslip inputs of ±2° at Mach 1.5. The data have

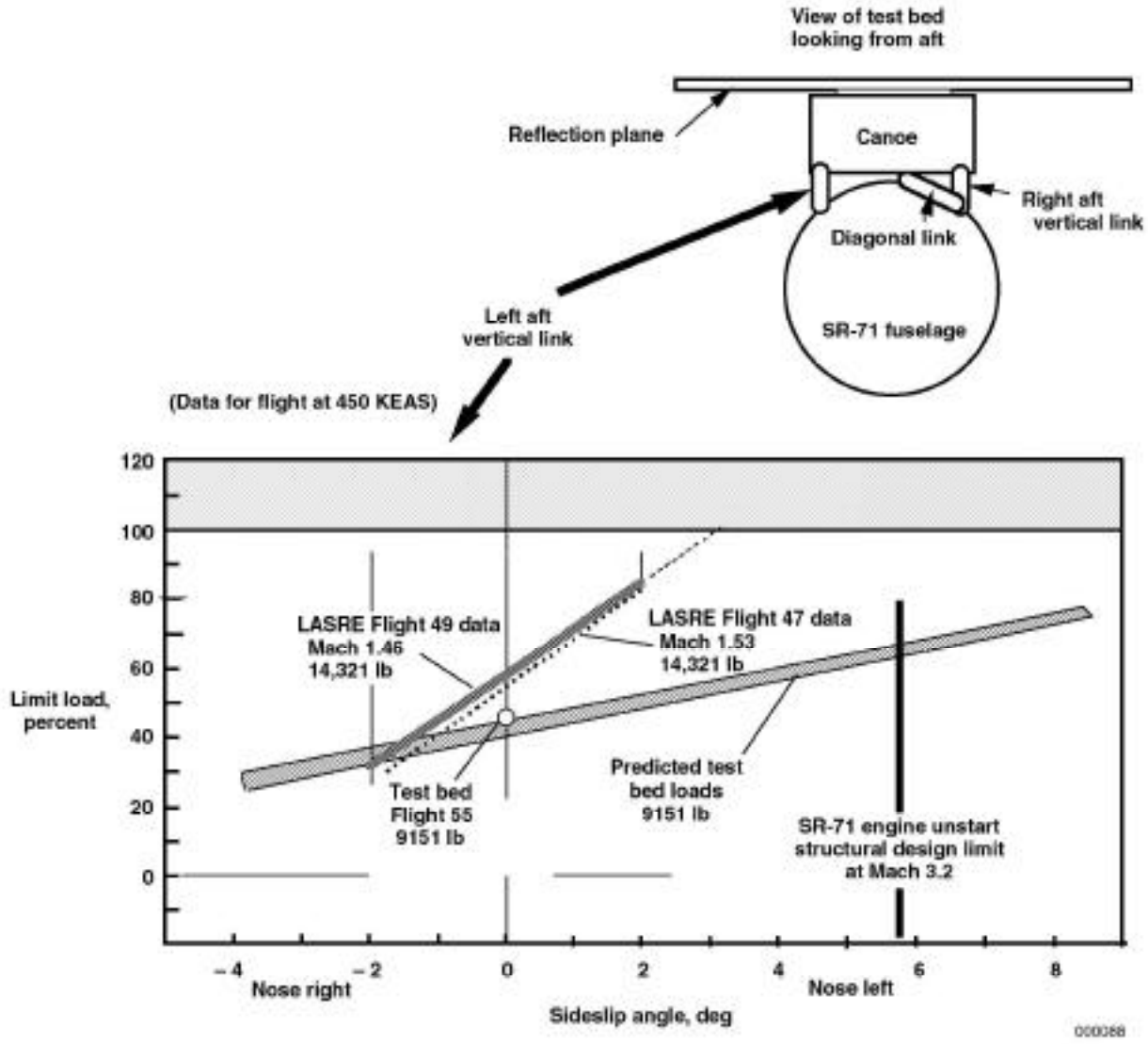

Figure 14. Canoe attachment point loads caused by sideslip (left aft vertical link).

been normalized to an airspeed of 450 *KEAS*. These data were used with “engine out” and “unstart” data from the SR-71 flight simulator to predict the LASRE load limits at high Mach numbers. Based on this analysis, LASRE flights were cleared to proceed to a speed of Mach 2.0 to obtain additional steady-state sideslip data; however, the program was terminated prior to reaching this cleared limit.

The test bed configuration resulted in significant reductions of load at the canoe attachment points as compared to the LASRE configuration (fig. 14). Figure 15 shows a comparison of the LASRE and test bed vertical surface area contributing to the side load. Aerodynamic side forces were assumed to be uniform over these side surface areas. With the LASRE model removed, both the side force and rolling moment about the reference axis were significantly reduced. The model weight removed was 4,300 lb, and an additional 800 lb of LASRE engine cooling water was not carried on these flights. Figure 15 shows the predicted loads for the test bed flights. The only test bed data point shown is at 0° angle of sideslip. The data point shown was in good agreement with the loads prediction.

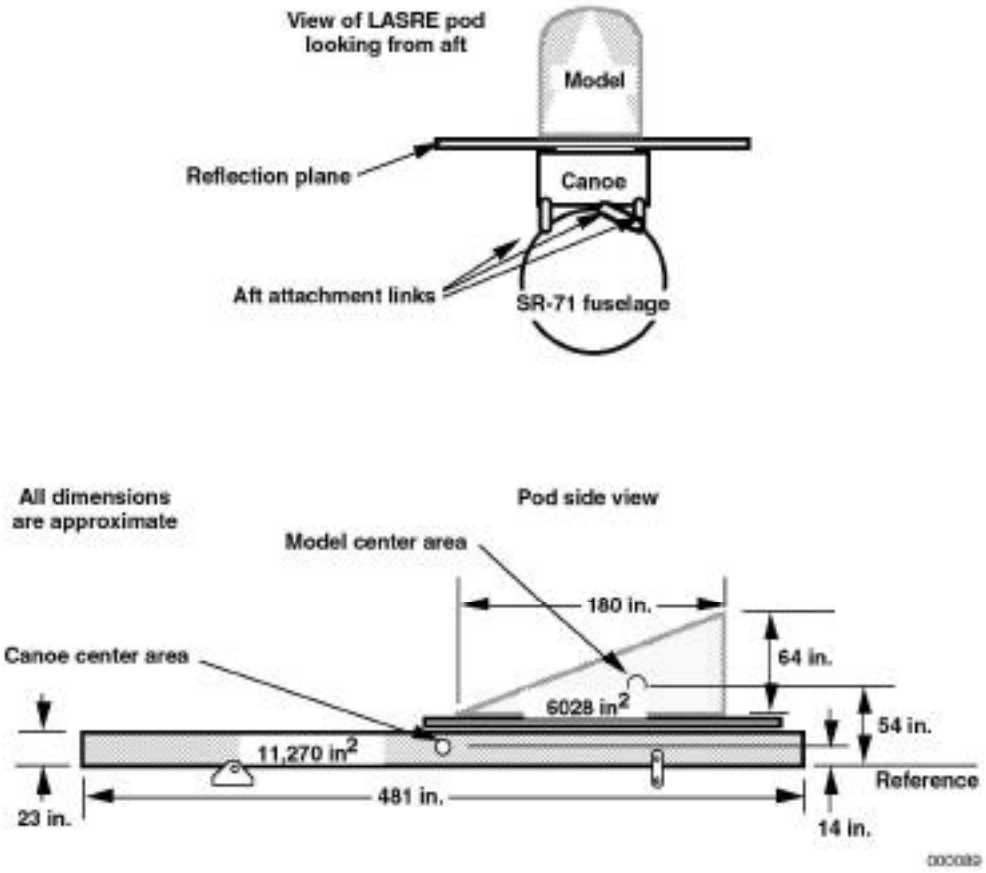

Figure 15. Comparison of LASRE and test bed vertical surfaces contributing to side load.

Based on SR-71 airframe structural limits (ref. 11), the temperature on the fuselage upper surface, underneath the canoe, is limited to 600 °F. Air temperature under the canoe was monitored at SR-71 fuselage stations 942 and 1135 during flights at speeds to a maximum of Mach 3. Projection of these data to Mach 3.2 indicate that temperatures would peak at approximately 500 °F. The test bed configuration was cleared to a maximum speed of Mach 3.2 without the need for further temperature monitoring.

Future test bed experiments will affect the loads at the mounting points to the SR-71 airplane and will have to be reviewed on a case-by-case basis. In general, longitudinal loads are less critical than vertical and side loads because the longitudinal design criteria is primarily based on an 8-*g* ultimate forward crash load for a 14,500-lb experiment. The longitudinal crash condition loads are large compared to any normal flight loads or thrust loads generated by probable experiments. Reference 11 should be used for general structural operating limitations for the design of experiments to be carried on the SR-71 test bed aircraft. In general, all experiment primary structure must be designed with a 2.25 factor of safety if the structural design is verified by analysis only, and with a 1.5 factor of safety if proof testing is to be performed to ultimate loads. If proof testing to other than ultimate loads is to be completed, a factor of safety between 1.5 and 2.25 may be used, pending NASA agreement.

Canoe Internal Environment

Flight test results for the canoe internal environment are presented. Results for the nitrogen purge effectiveness, fire detection, and canoe thermal environment are given.

Nitrogen Purge Effectiveness

Purge effectiveness has been evaluated in flight, primarily using data from the oxygen sensors. Figure 16 (ref. 12) shows data from a LASRE flight demonstrating the purge effectiveness. The canoe volume remains inert to less than 0.5-percent oxygen concentration from takeoff through subsonic cruise flight at altitude. Figure 17 shows similar results during a supersonic acceleration and climb. During descent, the altitude change is more rapid than during ascent. The purge system mass flow rate was not able to compensate for the air intrusion mass flow rate during this more rapid, ambient pressure increase during descent. Therefore, during descent, getting air intrusion caused by the ambient air pressure increase on the outside of the canoe is possible. A procedure used for the LASRE flights to avoid exceeding flammability limits during the descent phase was to dump propellants overboard and purge the experiment gas storage tanks before commencing the descent phase.

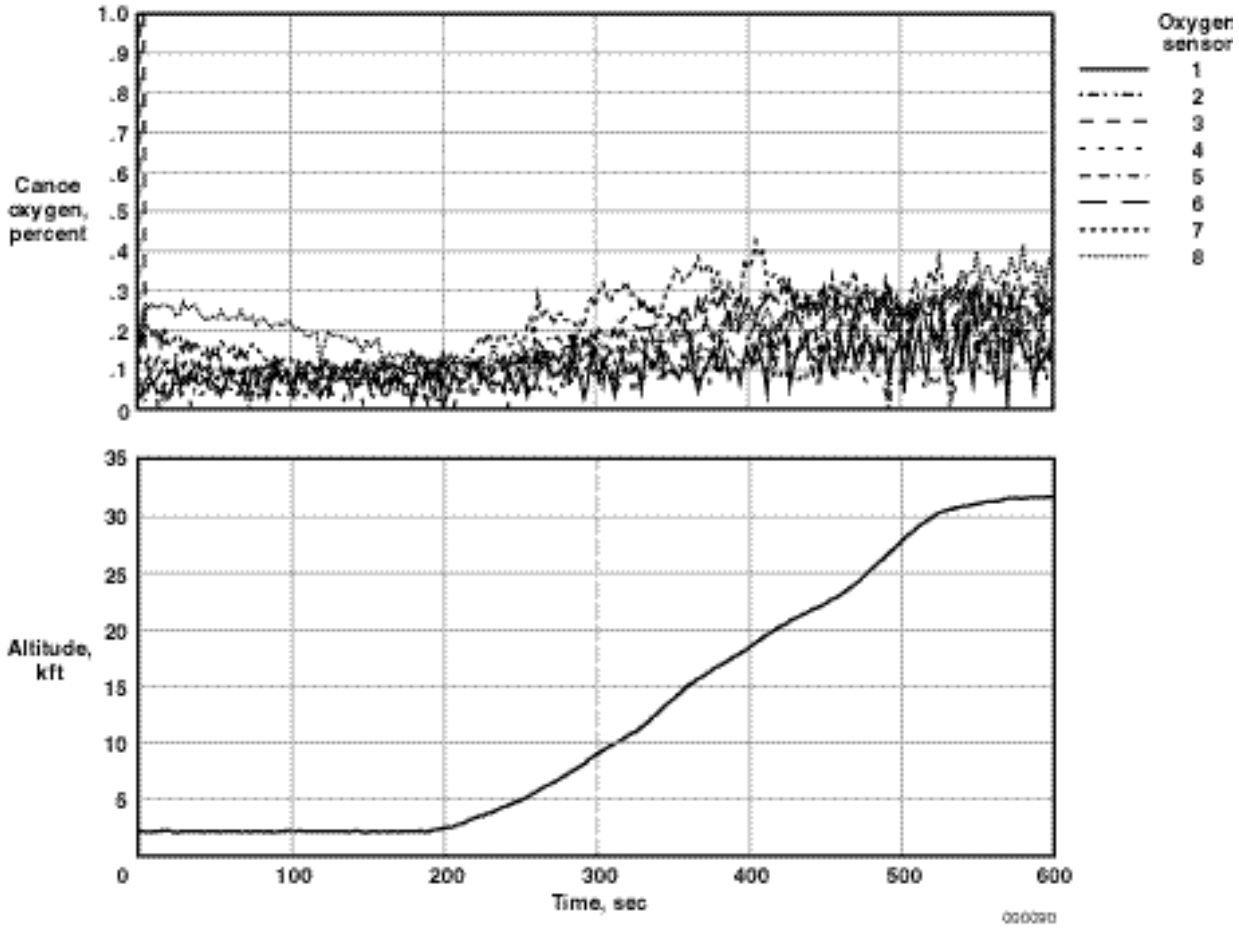

Figure 16. Oxygen levels with purged canoe; takeoff and subsonic cruise flight.

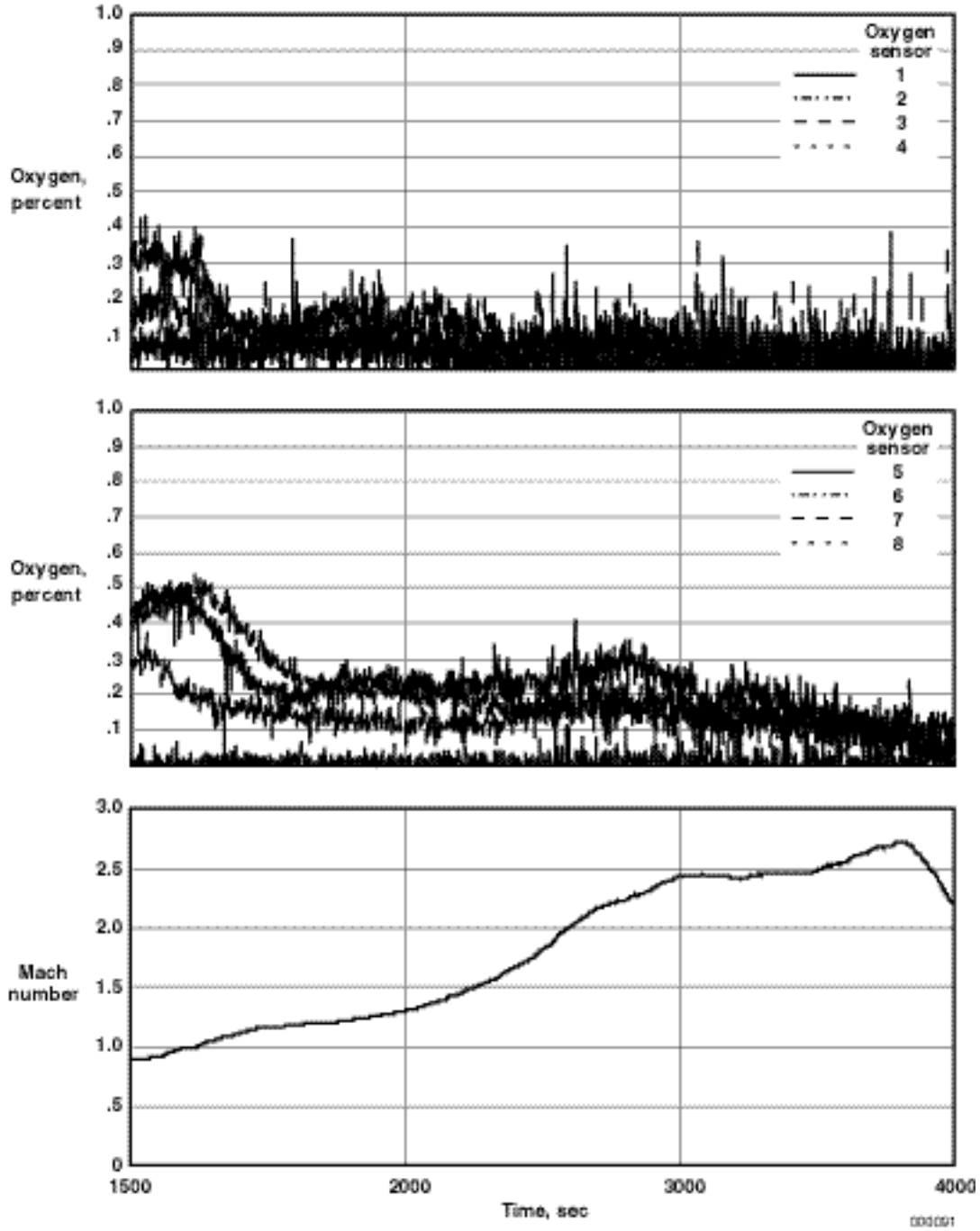

Figure 17. Oxygen levels with purged canoe; supersonic flight.

The purge also creates a pressurized environment, maintaining a positive pressure differential between canoe interior and the external ambient atmosphere. This positive pressure differential is maintained during ground operations, taxi, climb, acceleration, and steady cruise phases of flight. Figure 18 shows data for this pressure differential for a flight that reached an altitude of approximately 70,000 ft. The minimum pressure inside the canoe was approximately 4 lbf/in^2 atmosphere with a pressure differential of 3.3 lbf/in^2 at an altitude of 70,000 ft. The pressure differential can be regulated by a cockpit-controlled vent valve located at the aft end of the canoe. Overpressure protection is also provided by a large diameter relief valve that opens at 3 lbf/in^2 and is fully open at 5 lbf/in^2. The canoe structural design limit loads result in a maximum allowable pressure differential of 5 lbf/in^2.

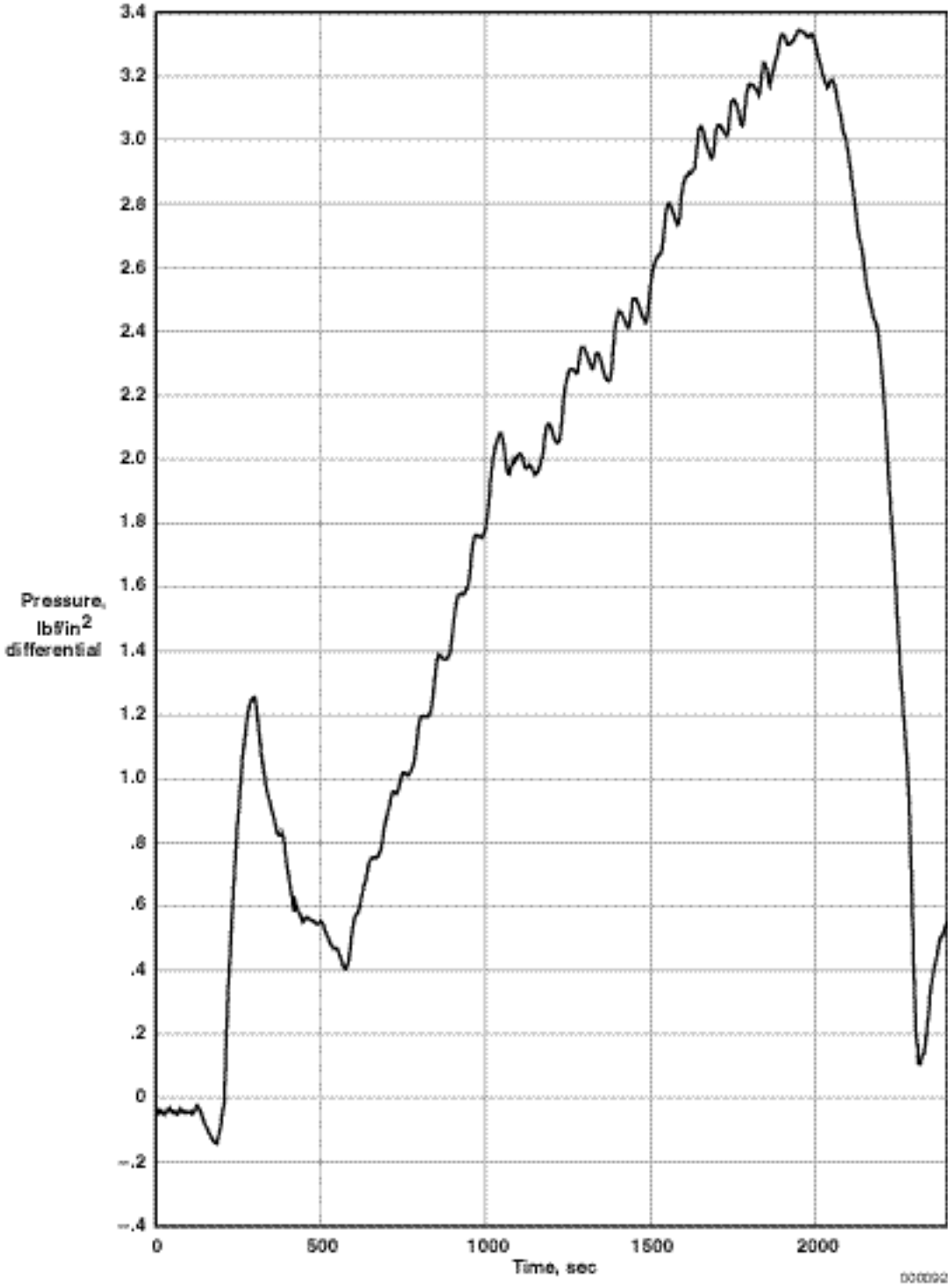

Figure 18. Pressure differential between canoe interior and atmosphere.

The purge also serves to slow the rate of overheating of canoe internal components, which can be important for supersonic Mach flight. The canoe internal temperature reductions, with the purge on instead of off, has not been quantified in flight.

Fire Detection and Canoe Thermal Environment

Figure 19 shows canoe interior temperature from the fire detection thermocouples for Mach flight to a maximum of Mach 3.03. Only approximately 15 sec of flight data were obtained. The peak temperatures lag the maximum Mach number by several minutes. Canoe internal temperatures as high as 160 °F are estimated to be likely if dwell times are extended to 1 min or longer at Mach numbers greater than 3.0. Localized temperatures may be even higher than 160 °F because of specific conduction paths through the structure.

During the test bed flights, an attempt was made to quantify the maximum temperatures of internal canoe structure and instrumentation pallet. Temperature indicator tabs were placed on the canoe steel structure at various locations and on the aluminum instrumentation pallet. The tabs provided an indication of the peak surface temperature attained on a given surface. The temperature tabs were installed after the second flight and not recorded until after the fourth flight (table 3). Therefore, the indicated peak temperature could have been reached in either the third or fourth flight.

Table 3. Canoe internal temperatures.

Area	Material	Maximum temperature, °F	Accuracy, °F
Canoe skin	Steel	375	±25
Canoe internal structure	Steel	275	±25
Instrumentation pallet	Aluminum	155	±5

The canoe is cooled primarily by the thermal inertial mass of the internal and external steel structure. Therefore, the maximum temperatures experienced by the structure during a flight will be a function of Mach number and the duration of exposure to supersonic Mach numbers. The cooling capacity of the purge is negligible when compared to this thermal inertial mass. Thus, the purge has little effect on the temperature of the steel structure and skin. However, the cool purge does mitigate the convective transfer of heat to instrumentation components.

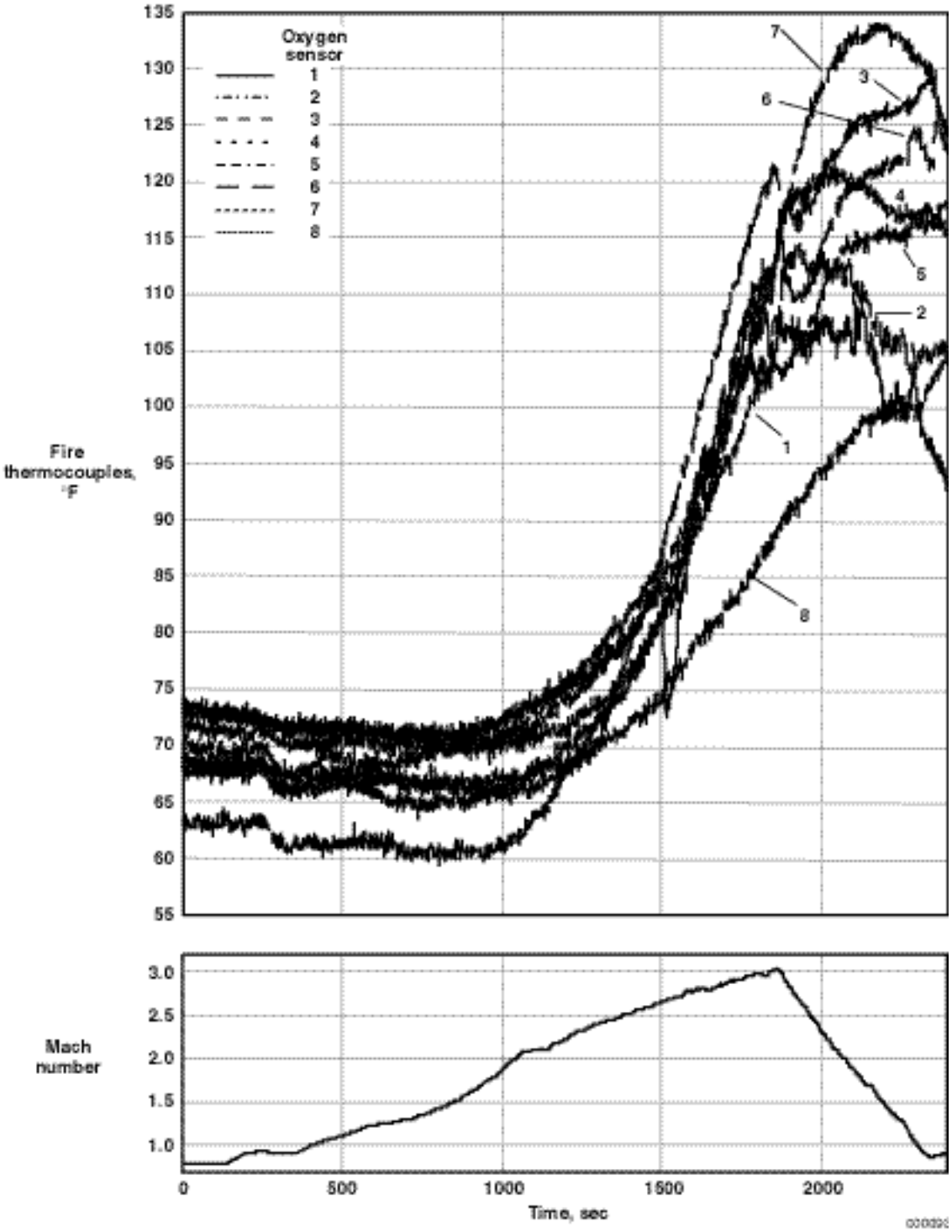

Figure 19. Canoe interior temperature data for supersonic flight.

Postflight temperature data were only obtained in the instrumentation pallet–main hydrogen valve compartment. However, the conclusions derived from this information are likely valid for the rear of the canoe. Table 3 shows the peak temperatures from the indicator tabs.

The difference between the 375 °F canoe skin peak temperature and the 275 °F peak temperature of nearby internal structure indicates that the room-temperature vulcanizing seal between the canoe skin and internal structure provided an effective heat conduction barrier. This seal was only intended for hermetic purposes and never intended as a heat conduction buffer. Future experiments may wish to incorporate an intentional conduction buffer to increase insulation. The maximum canoe internal structure temperature was observed near the attachment points to the canoe skin. However, several other internal structure measurements did not reach the 250 °F lower indicator limit of the temperature tabs, perhaps indicating that the structure did not reach a steady state.

The instrumentation pallet reached a peak temperature of 155 °F. This peak temperature was near the attachment points to the internal structure. Several other pallet temperatures were substantially lower. Little heat can be concluded to be conducted to the instrumentation pallet through the attachment structure. Convection from the surrounding gas probably was the main source of heating to the instrumentation equipment for the test bed flights. Thus, that the nitrogen purge be operated during supersonic Mach flight is important to mitigate this convective heat path. A thermal barrier between the instrumentation and structure also may be required for flights of longer duration in which heat soaking may be an issue.

Reflection Plane Flow Quality

For future air-breathing propulsion experiments carried on the SR-71 test bed, flow quality over the reflection plane into the inlet is anticipated to be important. For this reason, flow-field surveys were conducted at the location on the reflection plane where the inlet of an air-breathing engine might be placed.

Two flow survey rakes (fig. 20) were placed on the reflection plane. Longitudinally, the rakes were positioned as far forward as possible, but remaining behind the Mach wave from the leading edge of the reflection plane for Mach-3.2 flight. Laterally, the “centerline” rake was positioned 2 in. right of the

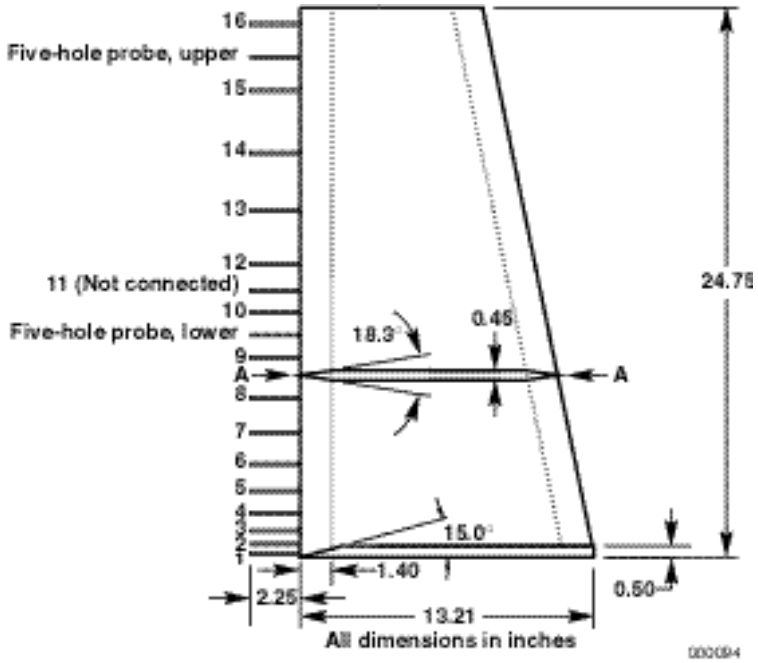

Figure 20. Reflection plane flow survey rakes.

reflection plane longitudinal centerline, and the “offset” rake was positioned approximately 17 in. left of centerline.

Each rake was 24.75 in. tall and had 16 total pressure probes. Each rake was fitted with two hemispherical-tip five-hole probes for flow angle measurements. These probes also incorporated static taps for instream static-pressure measurements. All pressure ports were measured with 10 lbf/in^2 differential scanning pressure sensors.

Static-pressure measurements were taken on the reflection plane at locations shown on figure 21. In the time available before flight, installing conventional flush static-pressure taps on the reflection plane was impractical. Therefore, thin stainless-steel tubes, sealed at one end, were glued to the reflection plane surface, and a hole was drilled at the measurement location. Measurements near the rakes provided local surface static pressures for the rakes. Upstream static-pressure ports provided some indication of upstream flow distortion.

Rake data were processed as follows: For subsonic flow, total pressure was equal to measured pitot pressure. Other flow parameters were calculated using compressible flow equations and then applying the average static pressure at the base of each rake uniformly over the entire rake, which is conventional practice for boundary-layer rakes. Although this assumption is not strictly valid in supersonic or free-stream flow, it was still found to be the best approach to obtain quantitative results from the available data. Static pressures from the five-hole probes appeared to experience substantial transonic effects and interference from neighboring probes, and therefore were not used. Only qualitative flow angle information was obtained from the five-hole probes; wind-tunnel calibration of the probes would be required to obtain quantitative data.

Figures 22 to 25 show representative flow-field data. Total pressures are presented rather than Mach number because for subsonic flow, total pressures are directly measured without using any assumptions, and because for low supersonic flow, the impact of assuming uniform static pressure across the rake is reasonable.

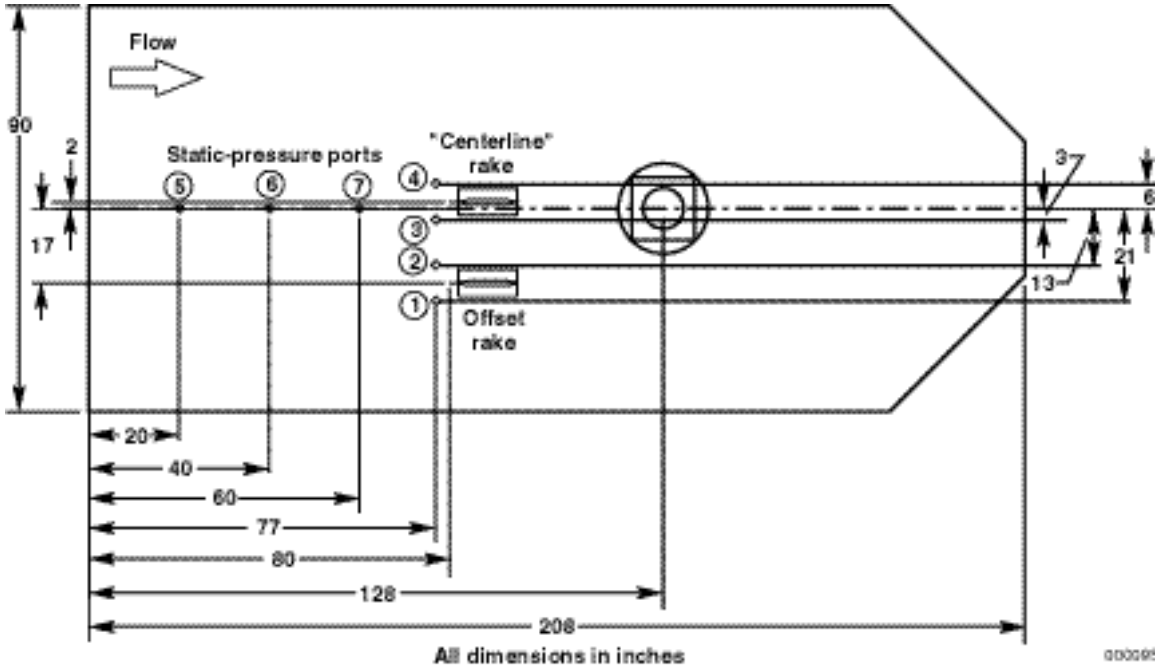

Figure 21. Location of flow survey rakes on reflection plane.

Figures 22(a) and 22(b) show total-pressure profiles at subsonic speeds; the flow field appears quite uniform. Figures 23(a) and 23(b) show the same for supersonic speeds; the flow is fairly uniform to a maximum of approximately Mach 1.6, but distortions substantially increase at Mach numbers greater than Mach 1.6. Figure 24 shows the average rake total pressure in the test region over a range of Mach numbers and in sideslip maneuvers. The total pressure decreases as Mach number increases and for right sideslip (nose right). Figure 25 shows the maximum minus minimum rake total-pressure distortions for these same test points. The flow distortions substantially increase for supersonic speeds greater than Mach 1.8 with no sideslip and for right sideslip.

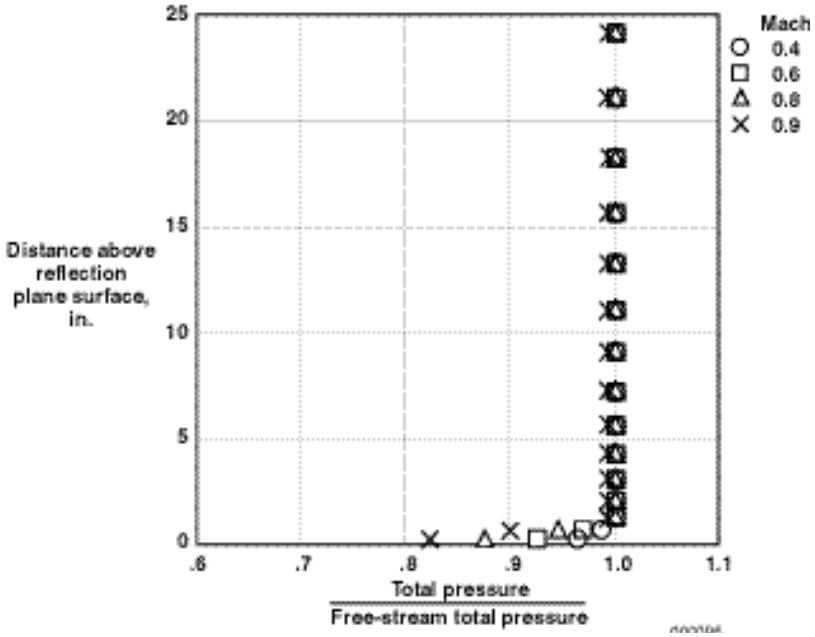

(a) Centerline rake total-pressure profiles.

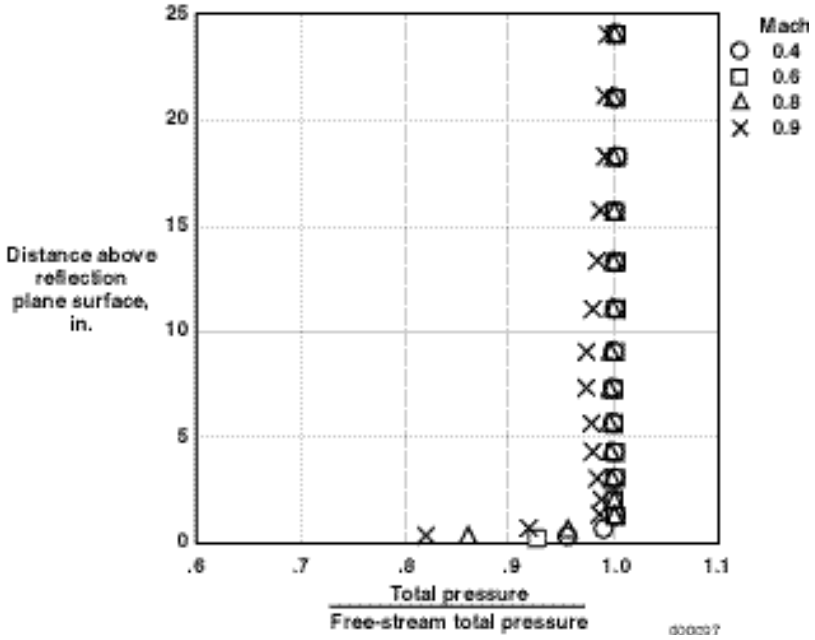

(b) Off-centerline rake total-pressure profiles.

Figure 22. Reflection plane flow data for subsonic flight.

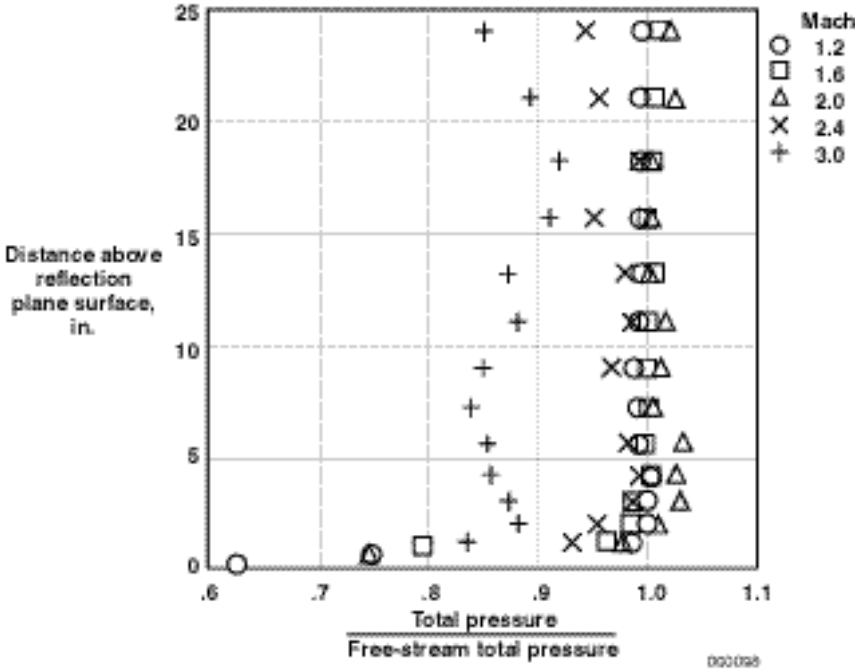

(a) Centerline rake total-pressure profiles.

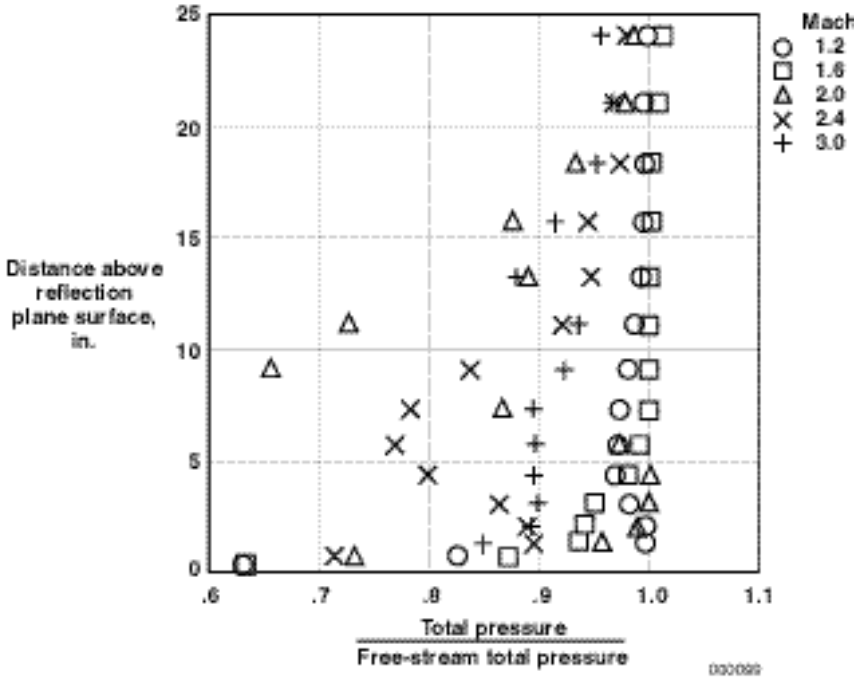

(b) Off-centerline rake total-pressure profiles.

Figure 23. Reflection plane flow data for supersonic flight.

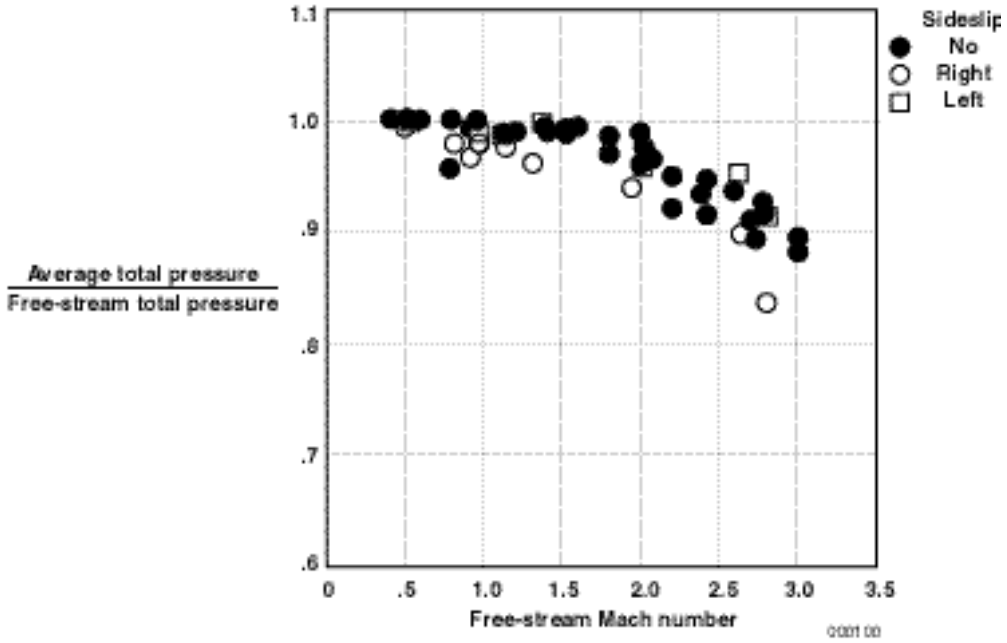

Figure 24. Reflection plane flow average total pressure.

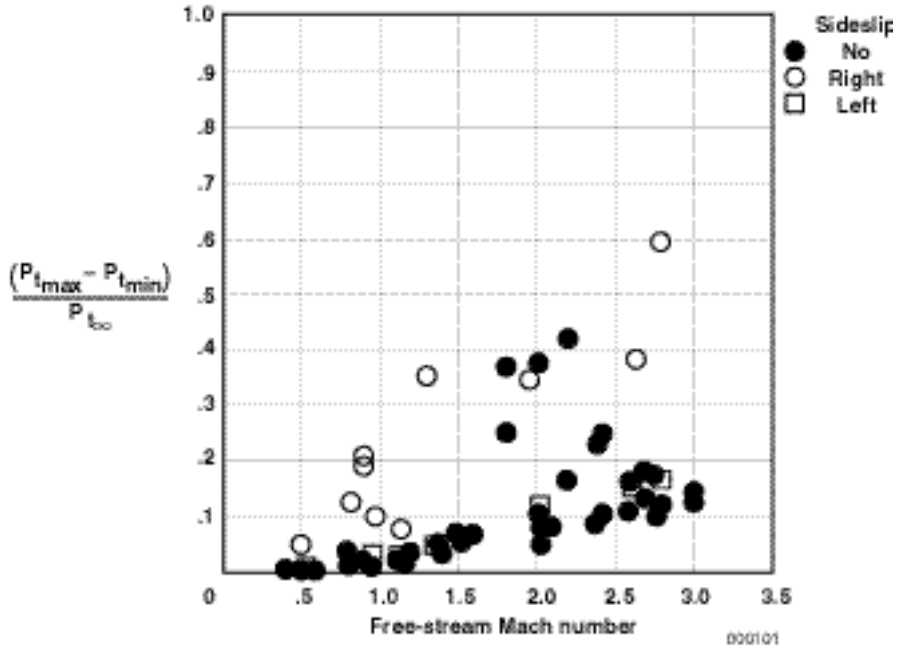

Figure 25. Reflection plane flow total-pressure distortion.

The reflection plane flow field appears quite uniform to a maximum of approximately Mach 1.6 in straight-and-level flight in the region surveyed. In sideslip, localized flow distortion exists in the potential test region. The distortion may be caused by vortices or wakes shed off the aircraft forebody or off the canoe forebody. Aircraft sideslip did not produce a uniform side wash over the test region. At speeds faster than Mach 1.6, variable pressure distortions were observed in the test region. These distortions may be caused by supersonic waves off the aircraft, possibly from the J58 engine inlets, cowl leading edge, or bleed exit ports. The boundary-layer thickness was no more than 2.1 in. at the rakes. Additional instream flow survey data may be required for specific experiments mounted on the reflection plane. Reference 12 provides further details of the data and analysis from the reflection plane flow survey flights.

SUMMARY

The SR-71 test bed aircraft configuration, composed of the canoe and reflection plane, has been described. Details of aircraft modifications, including structure, propulsion, and instrumentation, were given. Information concerning the design of SR-71 test bed experiments has been given in the appendix. Requirements have been summarized in the areas of aerodynamic characteristics and structural design. Additional standards have been provided for the design and carriage of pressure vessels and the requirements for ground testing.

Flight data have been presented to document the characteristics of the SR-71 test bed aircraft in support of using the facility for future test work. These areas include aerodynamics, stability and control, structural and thermal loads of the aircraft, and flow quality on the reflection plane. Information about the internal environment of the canoe has also been discussed.

Stability and control derivatives have been obtained from flight data for the Linear Aerospike SR-71 Experiment and test bed configurations. No longitudinal stability issues exist with either of these configurations. Directional stability and dihedral effect are reduced, but are acceptable for the configurations tested. Stability and control envelope expansion flights probably would be required for new experiments, although new wind-tunnel testing may not be required.

The existing structural modifications to the SR-71 test bed aircraft permit the captive-carry flight of external payloads of approximately 14,500 lb. Subtracting the 9,200-lb weight of the canoe and reflection plane, experiment weights of approximately 5,300 lb can be carried. The specific loads transmitted to the SR-71 fuselage will have to be analyzed for each experiment to guarantee the limit loads are not exceeded. The amount of sideslip that can be achieved for a particular experiment will also have to be determined for each experiment.

A nitrogen purge system has been demonstrated in flight to provide an inert atmosphere inside the canoe. This system can be used to help mitigate the hazards of carrying gases and liquids that react with oxygen.

The instream flow surveys of the flow over the reflection plane indicate that the flow is fairly uniform at subsonic and supersonic Mach numbers less than approximately Mach 1.5. Flow distortion is present at supersonic speeds greater than Mach 1.5 and in sideslip.

Dryden Flight Research Center
National Aeronautics and Space Administration
Edwards, California, April 5, 2000

REFERENCES

1. Corda, Stephen, Bradford A. Neal, Timothy R. Moes, Timothy H. Cox, Richard C. Monaghan, Leonard S. Voelker, Griffin P. Corpening, Richard R. Larson, and Bruce G. Powers, *Flight Testing the Linear Aerospike SR-71 Experiment (LASRE)*, NASA TM-1998-206567, 1998.

2. Lockheed Advanced Development Company, *Lockheed SR-71 Supersonic/Hypersonic Research Facility: Researcher's Handbook, Vol. II: Technical Description*, 1990.

3. Burcham, Frank W., Jr., Earl J. Montoya, and Phillip J. Lutschg, *Description of YF-12C Airplane, Propulsion System, and Instrumentation for Propulsion Research Flight Tests*, NASA TM-X-3099, 1974.

4. Pratt & Whitney, *J58 Thrust Upgrade Study for Hypersonic Air Launch Option Concept: Final Report*, FR-22741-1, Mar. 1993.

5. Conners, Timothy R., *Predicted Performance of a Thrust-Enhanced SR-71 Aircraft with an External Payload*, NASA TM-104330, 1997 (also published as ASME-95-GT-116, June 1995).

6. Mizukami, Masashi, et al., "Linear Aerospike SR-71 Experiment (LASRE): Aerospace Propulsion Hazard Mitigation Systems," AIAA-98-3873, July 1998.

7. Moes, Timothy R., Brent R. Cobleigh, Timothy R. Conners, Timothy H. Cox, Stephen C. Smith, and Norman Shirakata, "Wind Tunnel Development of an SR-71 Aerospike Rocket Flight Test Configuration," AIAA-96-2409, June 1996.

8. Moes, Timothy R., Brent R. Cobleigh, Timothy H. Cox, Timothy R. Conners, Kenneth W. Iliff, and Bruce G. Powers, "Flight Stability and Control and Performance Results From the Linear Aerospike SR-71 Experiment (LASRE)," AIAA-98-4340, Aug. 1998 (also published as NASA TM-1998-206565, 1998).

9. Maine, Richard E. and Kenneth W. Iliff, *Application of Parameter Estimation to Aircraft Stability and Control: The Output-Error Approach*, NASA RP-1168, 1986.

10. Murray, James E. and Richard E. Maine, *pEst Version 2.1 User's Manual*, NASA TM-88280, 1987.

11. Lockheed Martin Skunk Works, *LASRE Structural Criteria and Operating Limitations*, SP-7551, Rev. F, Nov. 1997.

12. Mizukami, Masashi and Daniel Jones, *Flow-Field Survey in the Test Region of the SR-71 Aircraft Test Bed Configuration to a Maximum of Mach 3.0*, NASA TM-209025, 2000.

APPENDIX
DESIGNING SR-71 TEST BED EXPERIMENTS

INTRODUCTION

Based on experience gained in designing and flying the Linear Aerospike SR-71 Experiment (LASRE) and test bed configurations, the following guidelines are being provided. Design philosophy, aerodynamics, structural design, pressure vessels, and ground testing requirements are addressed.

Design Philosophy

Because the experiment is to be captive-carried on the SR-71 manned aircraft, the experiment hardware and support systems must be designed to be single-fault tolerant (that is, no single failure may be catastrophic to the carrier aircraft). All components must be designed for four times the number of cycles required for completion of experimental testing (that is, ground and flight test).

Aerodynamics

As a minimum, any new experiment mounted on the SR-71 test bed will require stability and control envelope expansion flights. The amount of envelope expansion required probably would increase with the size of the new configuration. Wind-tunnel testing may not be required if the stability and control effects of the new configuration are evaluated to be bounded by the flight data available from the LASRE and test bed configurations.

Structural Design

All experiment primary structure must be designed with the following factor of safety, as appropriate:

- A 2.25 factor of safety, if structural design is verified by analysis only.
- A 1.5 factor of safety, if proof testing is to be performed to ultimate loads.
- If proof testing to other than ultimate loads is to be completed, a factor of safety between 1.5 and 2.25 may be used, if NASA concurs.

Pressure Vessels

All pressure vessels must be designed with the following factor of safety, as appropriate:

- The tank burst pressure must be 2.5 times the maximum operating pressure.
- The line proof pressure must be 1.5 times the maximum operating pressure.
- A leak test must be performed at the maximum attainable pressure.
- The maximum gaseous leak rate must not exceed 1×10^{-5} standard cm^3/sec.

Ground Testing Requirements

All emergency systems must be functionally checked on the ground, preferably with actual working fluids. Other ground testing, including leak checks, ground vibration testing, environmental testing, and so forth, will be determined after a detailed review of particular experiment hardware by NASA.

REPORT DOCUMENTATION PAGE

Form Approved
OMB No. 0704-0188

1. AGENCY USE ONLY (Leave blank)	2. REPORT DATE	3. REPORT TYPE AND DATES COVERED
	June 2000	Technical Publication

4. TITLE AND SUBTITLE

The SR-71 Test Bed Aircraft:
A Facility for High-Speed Flight Research

5. FUNDING NUMBERS

WU 529-70-14-00-12-00-PDE

6. AUTHOR(S)

Stephen Corda, Timothy R. Moes, Masashi Mizukami,
Neal E. Hass, Daniel Jones, Richard C. Monaghan,
Ronald J. Ray, Michele L. Jarvis, and Nathan Palumbo

7. PERFORMING ORGANIZATION NAME(S) AND ADDRESS(ES)

NASA Dryden Flight Research Center
P.O. Box 273
Edwards, California 93523-0273

8. PERFORMING ORGANIZATION REPORT NUMBER

H-2405

9. SPONSORING/MONITORING AGENCY NAME(S) AND ADDRESS(ES)

National Aeronautics and Space Administration
Washington, DC 20546-0001

10. SPONSORING/MONITORING AGENCY REPORT NUMBER

NASA/TP-2000-209023

11. SUPPLEMENTARY NOTES

12a. DISTRIBUTION/AVAILABILITY STATEMENT

Unclassified—Unlimited
Subject Category 02, 05, 07, 08

This report is available at http://www.dfrc.nasa.gov/DTRS/

12b. DISTRIBUTION CODE

13. ABSTRACT (Maximum 200 words)

The SR-71 test bed aircraft is shown to be a unique platform to flight-test large experiments to supersonic Mach numbers. The test bed hardware mounted on the SR-71 upper fuselage is described. This test bed hardware is composed of a fairing structure called the “canoe” and a large “reflection plane” flat plate for mounting experiments. Total experiment weights, including the canoe and reflection plane, as heavy as 14,500 lb can be mounted on the aircraft and flight-tested to speeds as fast as Mach 3.2 and altitudes as high as 80,000 ft. A brief description of the SR-71 aircraft is given, including details of the structural modifications to the fuselage, modifications to the J58 engines to provide increased thrust, and the addition of a research instrumentation system. Information is presented based on flight data that describes the SR-71 test bed aerodynamics, stability and control, structural and thermal loads, the canoe internal environment, and reflection plane flow quality. Guidelines for designing SR-71 test bed experiments are also provided.

14. SUBJECT TERMS

Flight test, SR-71 aerodynamics, SR-71 aircraft, SR-71 stability and control, SR-71 upper fuselage flow field, Test bed aircraft

15. NUMBER OF PAGES

39

16. PRICE CODE

34

17. SECURITY CLASSIFICATION OF REPORT	18. SECURITY CLASSIFICATION OF THIS PAGE	19. SECURITY CLASSIFICATION OF ABSTRACT	20. LIMITATION OF ABSTRACT
Unclassified	Unclassified	Unclassified	Unlimited